GEAR TECHNOLOGY

The Journal of Gear Manufacturing

MAY/JUNE 1989

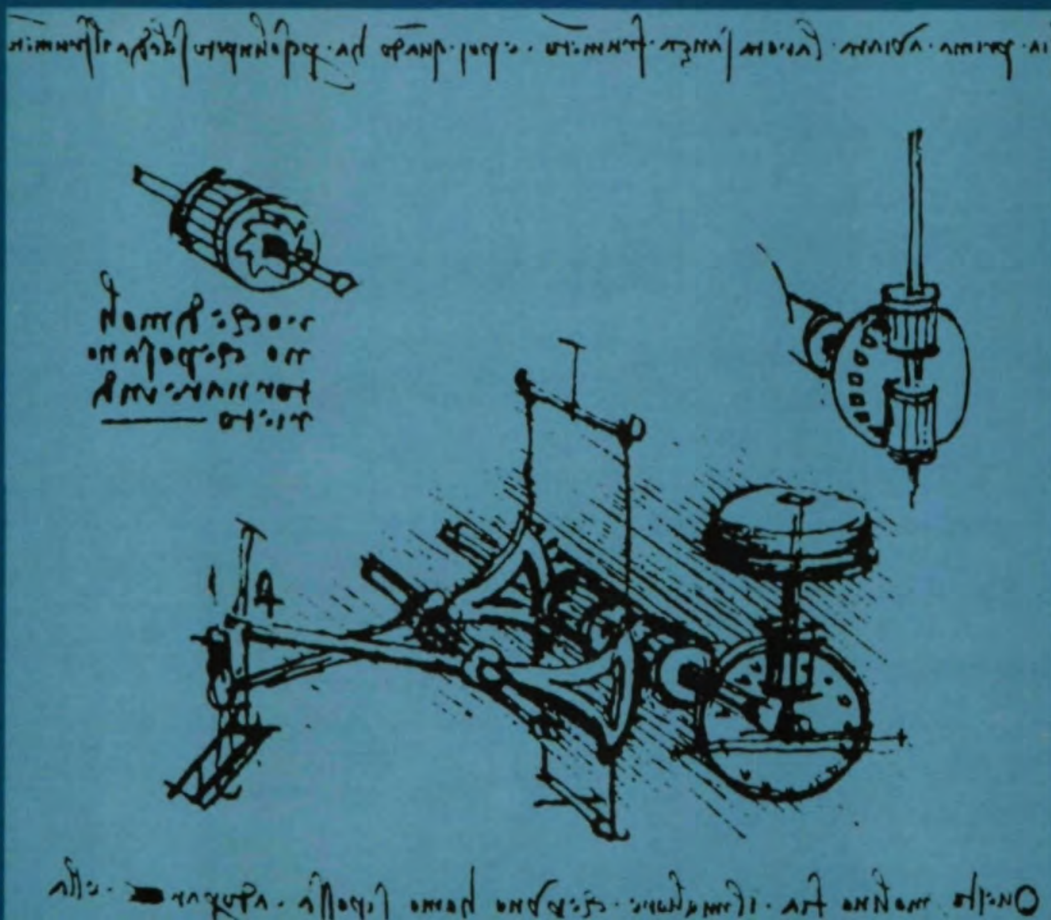

Testing of Cr-Free Carburizing-Grade Gear Steel

Gear Span Measurement

Into-Mesh Lubrication of Spur Gears—Part I

Form Diameter of Gears

Kapp makes fast work of high

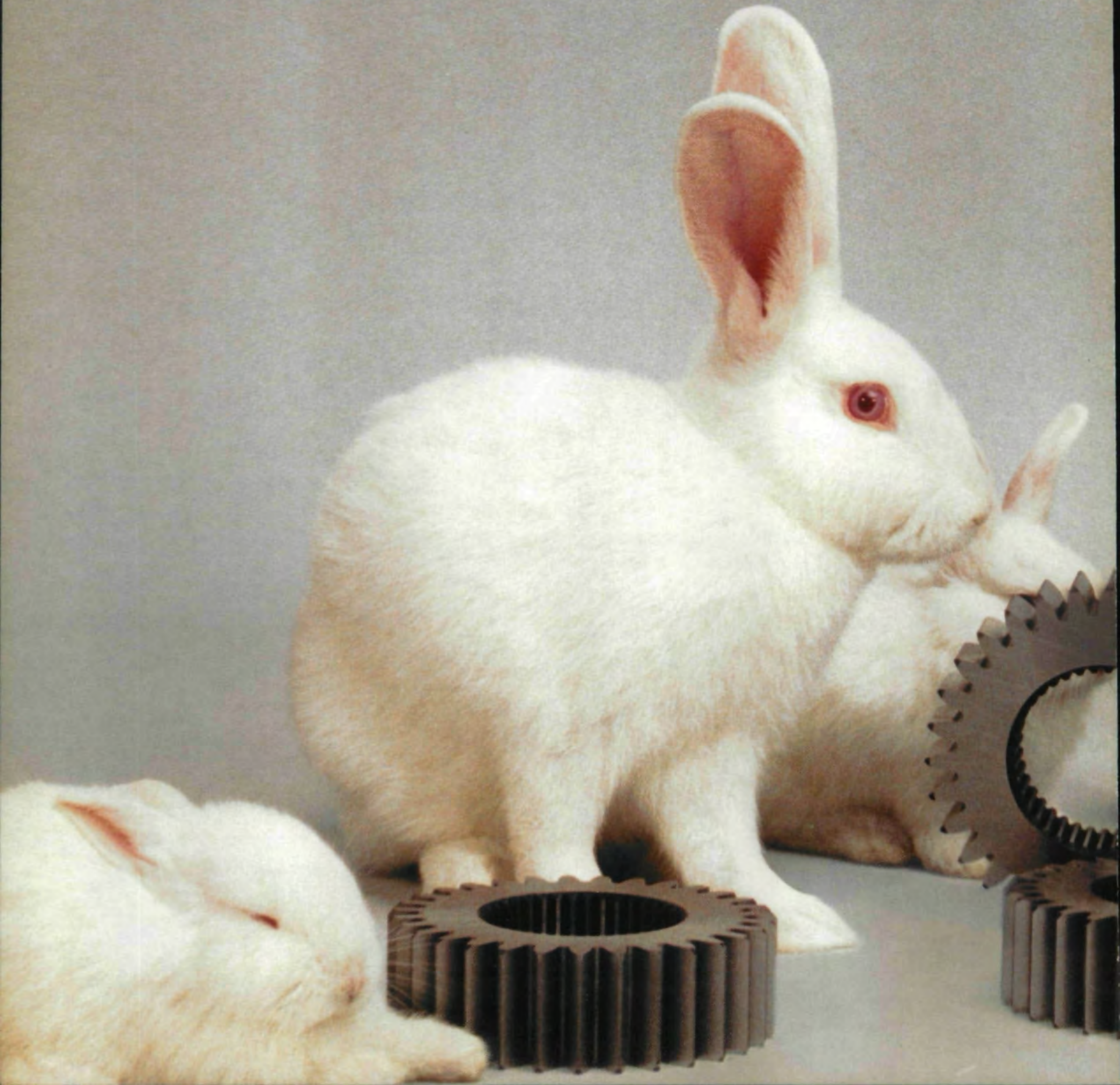

production jobs.

High production cutting of identical gear shapes requires both speed and accuracy. But some fast, accurate machines incur maintenance and operator costs that eat up profits. With Kapp CBN form grinding, you don't give up productivity to maintain profitability.

• Kapp CBN machines are faster than other grinding processes, with no heat checking or burning. Kapp CBN accuracy has proven itself on spur & helical involute forms, radial forms, near-net forgings, internal & external profiles, vane pump slots and constant velocity joints.

• Kapp CBN machines are operator friendly, for fast recall of setups and accuracy time after time.

• Kapp CBN machines use CBN wheels that incorporate the desired form right in the wheel with no need for dressing.

If you'd like to find out how Kapp CBN technology can improve your productivity, contact American Pfauter, 925 Estes Ave., Elk Grove Village, IL 60007. Phone (312) 640-7500.

CIRCLE A-1 ON READER REPLY CARD

RANDALL PUBLISHING
1401 Lunt Avenue
P.O. Box 1426
Elk Grove, IL 60007
(312) 437-6604

The Advanced Technology of Leonardo da Vinci 1452-1519

COVER

This design for a foot-operated grain mill is a variation on one of Leonardo's proposals for a windlass. In this machine, pumping the treadles seen in the assembly view at the center of the diagram sets the levers into alternate motion. This, in turn, makes the central shaft revolve and, through the crown gear, turn the millstone.

GEAR TECHNOLOGY
The Journal of Gear Manufacturing

CONTENTS

PAGE NO.

FEATURES

DEPARTMENTS

May/June, 1989 Vol. 6, No. 3

GEAR TECHNOLOGY, The Journal of Gear Manufacturing (ISSN 0743-6858) is published bimonthly by Randall Publishing Co., Inc., 1425 Lunt Avenue, P. O. Box 1426, Elk Grove Village, IL 60007. GEAR TECHNOLOGY, The Journal of Gear Manufacturing. Subscription rates are: $40.00 in the United States, $50.00 in Canada, $55.00 in all other foreign countries. Second-Class postage paid at Arlington Heights, IL and at additional mailing office.

Postmaster: Send address changes to GEAR TECHNOLOGY, The Journal of Gear Manufacturing, 1425 Lunt Avenue, P. O. Box 1426, Elk Grove Village, IL 60007.

MANUSCRIPTS: We are requesting technical papers with an educational emphasis for anyone having anything to do with the design, manufacture, testing or processing of gears. Subjects sought are solutions to specific problems, explanations of new: technology, techniques, designs, processes, and alternative manufacturing methods. These can range from the "How to . . ." of gear cutting (BACK TO BASICS) to the most advanced technology. All manuscripts submitted will be carefully considered. However, the Publisher assumes no responsibility for the safety or return of manuscripts. Manuscripts must be accompanied by a self-addressed, self-stamped envelope, and be sent to GEAR TECHNOLOGY, The Journal of Gear Manufacturing, P.O. Box 1426, Elk Grove, IL 60009, (312) 437-6604.

EDITORIAL

THIS FAR AND NO FARTHER

"They came first for the Communists, and I didn't speak up because I wasn't a Communist. Then they came for the Jews, and I didn't speak up because I wasn't a Jew. Then they came for the trade unionists, and I didn't speak up because I wasn't a trade unionist. Then they came for the Catholics, and I didn't speak up because I was a Protestant. Then they came for me, and by that time, there was no left to speak up."

Martin Niemoller

Thousands of miles from here, a political and religious leader has ordered a man killed. The Ayatollah Khomeini is offended by a book Salman Rushdie has written; therefore, he has decided this author must die. So what? Executions are ordered all the time in this world. The man who signed this order doesn't interest me. Neither does the book. It's all happening in another country. It has nothing to do with me.

But I am offended too—offended by the thought that one man can interfere with another's right to write what he pleases and with the rights of others to print, publish and distribute that work to those who wish to see it. As a publisher, I am offended that someone, for whatever reason, has attacked one of the foundation stones of a civilized society, the idea of research, inquiry and the free exchange of ideas.

Randall Publishing is a tiny enterprise compared with Viking Press, Mr. Rushdie's American publisher. We don't publish fiction, either tame or controversial. The idea of someone getting so worked up about an article in GEAR TECHNOLOGY that he or she would threaten me or the author seems patently absurd. At first glance, the whole Rushdie affair appears to be taking place on another plane. It appears that it has nothing to do with the business of researching and building gears or of publishing the results of that research.

But it does. Every publisher is in the business of ideas. Our job is to make ideas available to those who are interested in them. A threat to one of us becomes a threat to all of us. My name and the names of my colleagues go on the masthead. Every article is signed. If Mr. Rushdie is threatened into silence; if Viking Press can be threatened into not publishing a book; if bookstores can be threatened into removing certain books from their shelves, then none of us is safe.

All civilized society is based on the creative tension between the needs of the many and the needs of the few; between individual liberties and societal regulations. It consists of drawing a series of lines about certain behaviors and saying, "You can go this far and no farther," and then debating the placement of that line. On some issues, the line is very fine and flexible. We can afford to bend a little or a lot in either direction. On other issues, the line must be broad and immovable. The right to the free exchange of ideas is one of those issues.

The broad, immovable line on this issue seems to be drawn here: Any idea has the right to be made public where people can see it and evaluate it. There it will die or survive on its own merits. No one, but NO ONE, has the right to pre-censor an idea and decide for others whether it can be made public.

This is a difficult line to live with. It means, among other things, that we have to allow all the bad, false, stupid, demeaning, offensive and just plain silly ideas to stand right up there with the beautiful, the brilliant and the sublime. It means allowing ideas we find offensive to be published. It may mean defending people or ideas we personally find reprehensible.

There is no question that millions of people find Mr. Rushdie's book offensive. That is regrettable. But hundreds of thousands of books, pamphlets, periodicals and papers contain ideas offensive to *someone*. Must these all be withdrawn and their authors executed as well?

We cannot argue that because what is being offended are people's deepest personal religious sensibilities, a different set of rules must apply. The broad line does not bear tinkering with. If this week we can censor works of fiction, what is to prevent

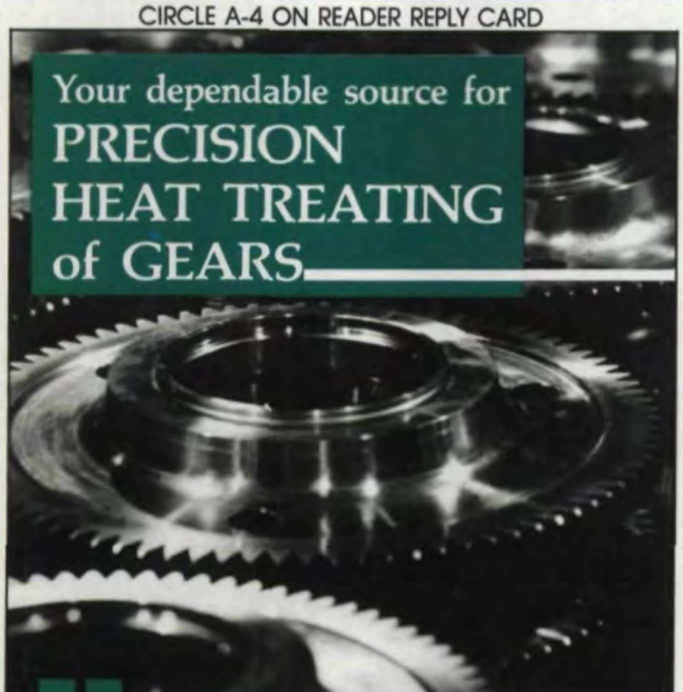

the censorship of political books next week and scientific books the week after that?

Nor does it do to brush off the whole Rushdie affair as being the result of a different cultural understanding or a different world view. The temptation to play Thought Police is not unique to cultures on the other side of the world. One of the most celebrated censorship cases in history did not involve a novelist or a political writer, but a scientist. It was Galileo, one of the finest scientific minds of the generation immediately following Leonardo's, that found himself in serious trouble with the law for publishing "offensive" scientific truth. Closer to our own time and our own culture, it is the scientific theories of Darwin that are among the most popular targets of those who would decide for all of us what is appropriate to read and think.

Dr. Samuel Johnson once said, "When a man knows he is to be hanged in a fortnight, it concentrates his mind wonderfully." In that sense, the death threat against Salman Rushdie has probably been a good thing for those of us in the business of disseminating ideas. Used to the polite legal dance in which censorship forces in the U.S. engage, we tend to forget exactly the kind of stakes we are playing for. The Rushdie affair has reminded us.

Whether we are writing and publishing innocuous gearing journals or controversial books on the cutting edge of research and thought, trading in ideas can be a dangerous business. Ideas *can* change the world. They can also kill people. Yet it is this trade in ideas that makes progress of all kinds possible.

In the West, developing custom over the past centuries has taught us to be a bit careless of the grounding of this free exchange. We have come to take it for granted. It's not that censorship does not exist here, but rather that its enforcement tends to be selective, limited by legal constraints and softened by custom. Now the Ayatollah has cut through all that to the heart of the matter. He has reminded us again that the foundation stones on which the idea of free inquiry is based are fragile. It takes only one man or one terrorist act to threaten the rules by which we all play.

The right of free expression is one which applies either to everyone or to no one. The threat to limit that right for anyone, no matter how far removed from our own field of interest or how objectionable his ideas, is, ultimately, a threat to all of us. If we value the principles of free inquiry and the free exchange of ideas, we must say at this time, over this book, regardless of its literary, political or religious merit, "If this author is silenced, we are all silenced. Here is where we draw the line."

Michael Goldstein

Michael Goldstein, Editor/Publisher

TECHNICAL CALENDAR

MAY 18-21. AGMA Annual Meeting, "The Changing World of Gears." Loews Ventana Canyon Resort, Tucson, AZ. Panel discussion on unification of European Common Market in 1992. Keynote address on change management for industry. For more information, contact: Jill Burnett, AGMA, 1500 King St., Suite 201, Alexandria, VA, 22314. (703) 684-0211.

JULY 12-14, 1989. ASM International Conference on Carburizing. Sheraton Hotel & Conference Center, Lakewood, CO. Tech conference for heat treaters, gear manufacturers, users of carburized metals. For more information, contact: ASM International, Metals Park, OH, 44073. (216) 338-5151 or fax (216) 338-4634.

SEPTEMBER 12-20, 1989. European Machine Tool Show, Hannover, West Germany. Exhibits from 36 countries will show cutting and forming equipment, machine tools, CAD/CAM, robotics, etc. For more information, contact: Hannover Fairs, USA, Inc., 103 Carnegie Center, Princeton, NJ, 08540. (609) 987-1202.

NOVEMBER 6-8, 1989. AGMA Gear Expo '89, David Lawrence Convention Center, Pittsburgh, PA. Exhibition of gear machine tools, supplies, accessories and gear products. For more information, contact: Wendy Peidl, AGMA, 1500 King Street, Suite 201, Alexandria, VA, 22314. (703) 684-0211.

NOVEMBER 7-9, 1989, AGMA Fall Technical Meeting, Pittsburgh, PA. Seminars on a variety of gearing subjects held in conjunction with Gear Expo '89.

AGMA TECHNICAL EDUCATION SEMINARS. AGMA is offering a new series of technical education seminars, each one focusing on a different aspect of gear manufacturing and taught by industry experts.

May 2, Cincinnati, OH. "Gear Math at the Shop Level for the Gear Shop Foreman."

June 6, AGMA Headquarters. "Specifying and Verifying Material Quality per AGMA Material Grades."

June 6-7, 1989. Cleveland, OH. "Source Inspection of Loose Gears From the Customer's Standpoint." Second session. By request, a repeat of this seminar is being held. Here's your chance to get in on this popular seminar.

For more information, contact: Bill Daniels, AGMA, 1500 King St., Suite 201, Alexandria, VA, 22314. (703) 684-0211.

Matrix CNC Thread Grinders...

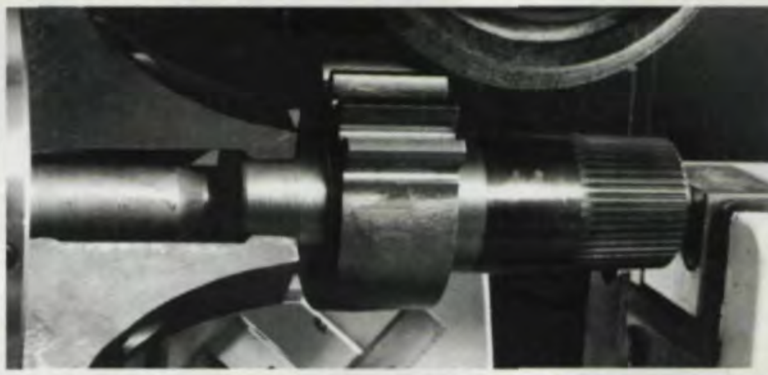

...Dramatically Slash Production Time!

CNC Thread Grinders from Matrix can drastically reduce your production time. Programmable control of infeed and auto-grind cycle, plunge grinding cycles and dressing, combined with the largest family of thread grinders in the world, make Matrix the logical choice to solve your grinding problems regardless of material or application.

Appropriate to a multitude of applications, Matrix CNC Thread Grinders are ideal for ball screw production, internal and external A. P. I. grinding, worm grinding, micrometer and surgical screw production, grinding the tracks in recirculating ball nuts, and many more. These Matrix machines can handle almost any aspect of precision grinding.

	1600 Series	4750 Series	5750 Series	6900 Internal	7000 Lg. Capacity
Swing over table ways	8"	15"-75"	15"-75"	19"	15.5"
Distance between centers	18"	49"	90"	-	197"
Maximum ground length.	8"	41"	78"	118"	161"
Maximum ground diameter	8"	12.5"	12.5"	10"	10"
Grinding wheel diameter	14"	-	20"	1" to 5"	20"
HP of wheelhead drive	5 and 7½	10, 20 or 25	10, 20 or 25	5	10, 20 or 25
Helix of wheel, LH & RH	20°	45°	45°	10°	24°
Workhead thru bore	1.5"	3.97"	3.97"	N/A	6⅛"

Internal or external threads of virtually any form, single or multi-start, right or left hand, parallel or tapered can be easily ground with or without relief. It only takes the right Matrix CNC Thread Grinder for the Job.

Choices of wheel dressing units are available in conventional template or dresser arm style, diamond roll, crush roll plus a versatile CNC Dress Unit.

Several of the more popular Matrix thread grinding models are shown in the table at left. Details on other models available can be obtained by writing or calling Matrix-Churchill Corporation, 5903 Harper Road, Solon, Ohio 44139 or 216/248-7950. FAX 216-248-7981.

MATRIX-CHURCHILL

CIRCLE A-8 ON READER REPLY CARD


SERIES EE

Production Testing of a Chromium-Free Carburizing Grade Gear Steel

D.H. Breen
ASME Gear Research Institute, Naperville, IL
T. Cameron
J.M. Ney Company, Bloomfield, CT

AUTHORS:

DALE H. BREEN *is Secretary and Director of ASME-Gear Research Institute. Prior to taking this post, he worked for sixteeen years for International Harvester Company, managing the corporate metallurgical research laboratories. His technical interests include gear technology, fatigue and fracture of metals, alloy steel and iron technology, tribology, and mechanics. Mr. Breen did undergraduate work in mechanical engineering at Bradley University, Peoria, IL. He holds a MS degree in metallurgy from the University of Michigan and a MBA from the University of Chicago. He is the author of numerous books and papers on gears, metallurgy and fatigue and is a member of ASM, ASME, SAE, ASLE and the American Institute of Mining and Metallurgical Engineers.*

DR. TOM CAMERON *is presently employed by J.M. Ney, Bloomfield, CT. At the time of the writing of this paper, he was on staff of AMAX Research and Development Center, Golden, CO, working on process development for wrought aluminum products. Prior to this assignment, he spent five years at AMAX's Ann Arbor, MI, center, working on alloy development of low alloy carburizing steels. This research was directed toward gearing applications and the relative roles of alloying and processing in gearing performance, and it led to the development of a combined overload-plus-fatigue test for carburized components that would determine the load at which cracking occurred in the case. Dr. Cameron earned his PhD from the University of Connecticut for research conducted on the Fe-B-C system.*

Fig. 1 – Power circulating gear test rig. Test gears are on the left.

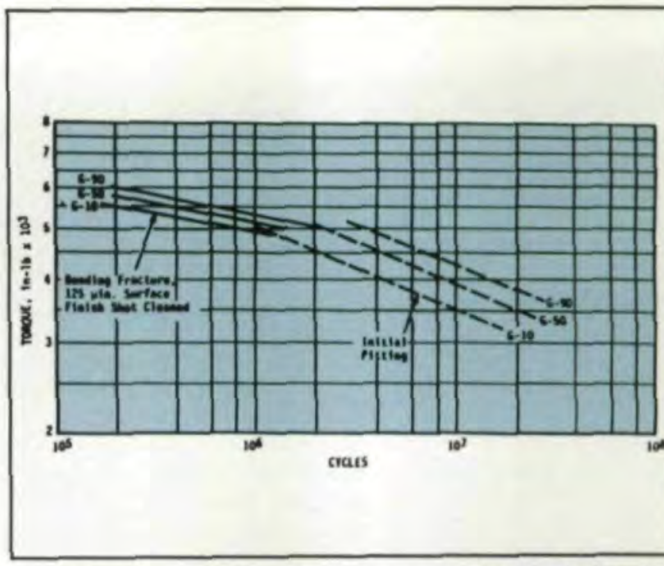

Fig. 2 – Torque vs. cycle life curves of the comparison data base developed by International Harvester from circulating gear tests.

Abstract:

The results of Bureau of Mines sponsored research under Contract #J0145009 to evaluate the manufacturing and engineering performance of a new chromium-free gear steel are reported. This material was developed under BOM Contract #J0113104. Since most chromium is imported from politically unstable regions of the world, alloys have been developed for contingency purposes. Gears were tested in a power circulating device to evaluate their strength (bending) and durability (pitting) characteristics for comparison with an existing data base. Selected samples were compared in terms of microstructure, cleanliness, grain size, x-ray retained austenite and x-ray residual stress. The new steel was shown to be comparable to 8620, the popular high-tonnage gear steel it was designed to replace.

Introduction

For many years chromium has been a popular alloy for heat treatable steels because of its contribution to hardenability more than offsets its costs. As a consequence, it is specified in such high-tonnage steel grades as the 5100, 4100 and 8600 series; and, as a result, about 15% of the annual U.S. consumption of chromium is used in constructional alloy steels.

Chromium is also a strategic alloy because it enhances corrosion and heat resistance of critical aircraft components. The United States imports most of its chromite ore and, unfortunately, much of this important material comes from politically unstable regions of the world. In fulfilling their responsibility to assure an adequate supply of strategic alloys, the Bureau of Mines has sponsored research to develop substitute material systems where feasible. In the first part (Phase I) of research with this aim, candidate substitute non-chromium bearing compositions were developed as potential replacements for 8620 and 4100 steels. The results of the alloy development phase were reported previously by Sharma and Keith.[1] This earlier work was accomplished utilizing a computer based alloy steel design system known as CHAT (Computer Harmonized Application Tailored).[2] The basic principle of the CHAT system is that steels will respond to heat treatment alike; i.e., develop the same microstructures if they have equivalent hardenabilities.

For carburizing grades, equivalent hardenability includes both case hardenability (D_{Ic}) and base hardenability (D_{Ib}). Other important considerations are carbon content and residual stress. Residual stress is thought to be controlled in part by martensite start (Ms) and martensite finish (Mf) temperatures; hence, a change in the alloy system should be kept minimal in order not to influence adversely residual stress. The aim is to calculate, by a computerized method, compositions which will have the same response to heat treatment, hardness and residual stress. A unique aspect of the system is that steels may be designed on a least-cost basis, since cost can be made an objective function. This system has been utilized successfully in developing steels for a number of specific applications and several of the SAE EX steel grades.

In the previous work reported in 1983, a five-year alloy cost projection was made. These costs were used as computer input with least-cost-without-chromium being a primary constraint. The cost projections turned out to be inaccurate; however, the relative costs are similar. Hence, the compositions developed still represent cost-attractive systems if chromium is not available. They are manganese-molybdenum (Mn-Mo) and manganese-molybdenum-nickel (Mn-Mo-Ni) systems. Of equal importance, this work has given another opportunity to confirm the concept that substitute steels having equivalent performance can be designed using fundamental metallurgical considerations.

In industry, however, performance concepts have not matured to the point where substitutes are readily accepted without back-up testing. In the real world, experience has not always justified theory. A great deal still remains to be learned (and unlearned) about alloy effects themselves, variations in nonmetallics, tramp elements, etc. Myths and illusions are not uncommon in the industrial community, and encumbent materials are highly favored. Substitute "ready" systems have to be validated with at least a limited amount of performance data before they will be accepted.

The aim of the work reported herein was to "prove-up" the new steel compositions in terms of their production, processing and performance characteristics. Based on tonnage and the fact

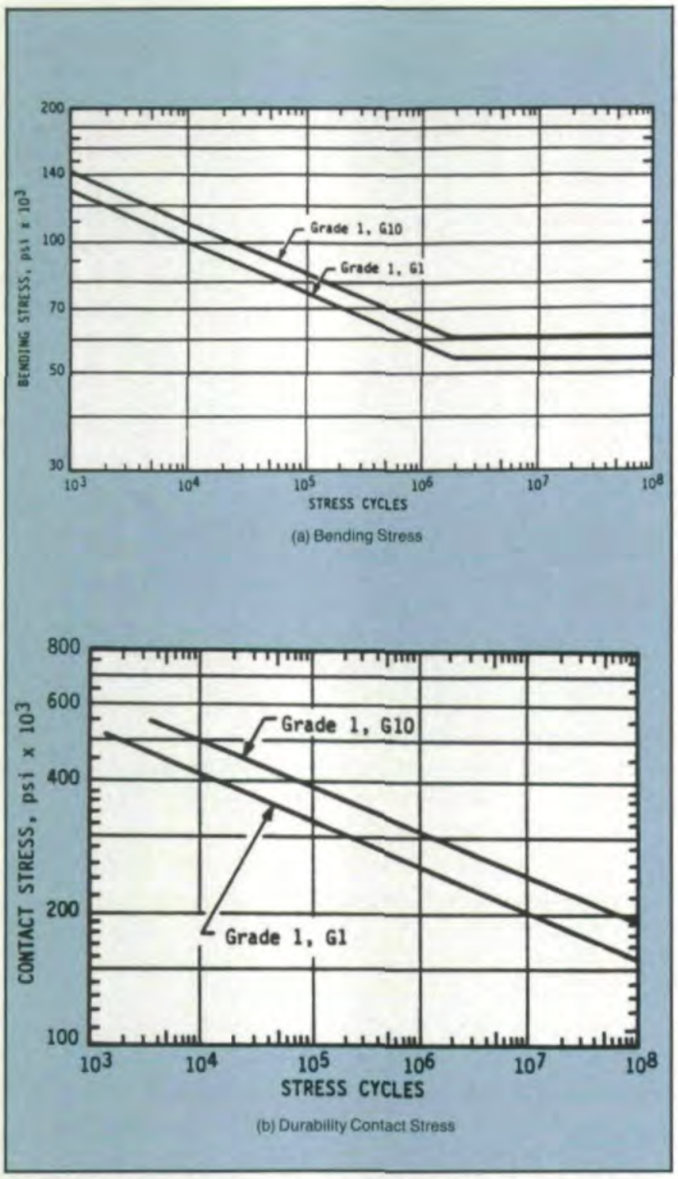

Fig. 3 – AGMA allowable stress curves for strength bending stress and durability contact stress.[5]

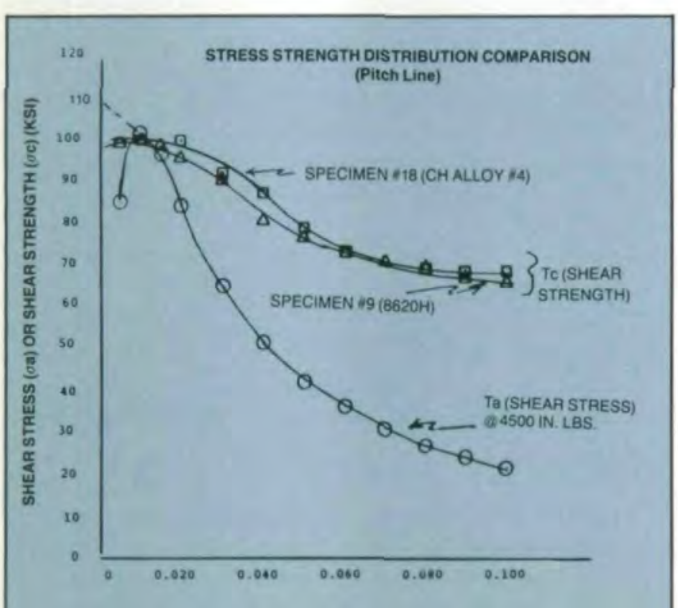

Fig. 4 – Gradient strength analysis.

that carburized applications are more complex, an 8600 equivalent from the Phase I work was chosen for evaluation. Based on cost, a Mn-Mo composition was selected to produce prototypes and specimens for tests. Its composition is shown in Table 1 in conjunction with the 8620 used as the control group. It was purposely produced with Mn to the high side since high-manganese steels have been an ongoing concern in the domestic industry. These types of steels are used, however, in high tonnages in Europe.

TABLE 1
CHEMICAL ANALYSIS (Wt%)

ELEMENT	EXPERIMENTAL ALLOY Cr free			CONTROL ALLOY 8620-H		
	SPECIFIED	HEAT ANALYSIS	SPECIMEN ANALYSIS	SPECIFIED	HEAT ANALYSIS	SPECIMEN ANALYSIS
Carbon	0.16/0.21	0.19	0.21	0.18/0.25	0.18	0.19
Manganese	1.00/1.30	1.29	1.27	0.70/0.90	0.73	0.73
Phosphorous	0.035 max	0.011	0.02	0.035 max	0.005	0.01
Sulphur	0.040 max	0.010	0.01	0.040 max	0.026	0.03
Silicon	0.15/0.35	0.26	0.25	0.15/0.30	0.22	0.22
Nickel	–	0.034	0.04	0.40/0.70	0.51	0.53
Chromium	–	0.055	0.06	0.40/0.60	0.49	0.45
Molybdenum	0.35/0.45	0.41	0.42	0.15/0.25	0.19	0.19
Aluminum		0.05	0.05			0.03

The strategy in this present endeavor was to produce prototype gears for evaluation using near-commerical procedures. Details concerning steel production, forging, machining and heat treat are given in a report by the Bureau of Mines authored by T. Cameron [3] and will not be repeated here. The material came from a 10 ton heat of steel. Gears were selected for evaluation, since they are critical components. They are sensitive to variations in steel quality, and gear performance data can be used as a basis for judgment concerning many other machine elements. Such properties as fatigue, both bending and contact, adhesive wear and surface finish are all incorporated into the design considerations for gears.

The work reported herein had as a major objective validation of the equivalency of computer-designed Cr-free and 8620 steels. This objective was accomplished principally by comparing the strength (tooth bending fatigue) and durability (flank pitting fatigue) of gear specimens. The pinion gear specimen was a 6P, 18T, 20° PA system with 3.3″ OD. Its mate was a 30T, 5.3″ OD gear. Fig. 1 shows the gear set installed in a power circulating (PC) gear test rig. This gear set and test method was selected because of the availability of an existing data base.[4] This data base, shown in Fig. 2, was generated over a number of years in the laboratories of International Harvester Company and has been expanded with additional tests at the ASME Gear Research Institute. Another important source of gear performance data is the allowable stress curves published by AGMA[5] for design use. These curves for bending and contact are shown in Figs. 3a and 3b.

In addition to performance testing, several other comparisons were made. They included continous cooling transformation (CCT) characteristics, hardenabilities, gradient hardnesses, microstructures (case and core), grain size, grain flow direction, residual stress, distortion in heat treat, inclusion ratings, dimensional accuracy and surface finish.

Results

The Cr-free test gears and the control group of 8620 gears were processed as a group through the same equipment. The control group was used to calibrate the data base. This precaution was taken since gear performance is sensitive to small variations in metallurgy, surface finish and geometry.

Only the most pertinent of the above comparisons are reported here. The reader is referred to the official Bureau of Mines publication mentioned earlier for additional details.

Gradient Strength

Gradient strength, a critical design consideration, is important to prevent failure by subcase fatigue. This property was not evaluated in this study, since subcase fatigue will not occur if a sufficient gradient strength is provided. Gradient strength is comprised of a combination of case depth and core hardness. Previous studies [6-7] indicate that steels with hardenabilities similar to those used in this work, when properly carburized, develop adequate gradient strengths in heat treatment with this size gear. As a check, however, a strength/stress distribution analysis was conducted near the pitch line. The results of this analysis are shown in Fig. 4. The comparison was made for a load of 4600 lb-in. torque. As can be seen, both steels provide more than adequate gradient strength to prevent failure at the case/core fracture.

Metallurgical Considerations

The Jominy hardenability test and the CCT diagram determination are two different ways of evaluating the transformation sequence that occurs when cooling a piece of steel. The objective of Phase I of this program was to develop a composition that would have similar hardenability to 8620. The hardenability testing conducted in Phase I of this program was more extensive than that conducted in Phase II. Sharma and Keith conducted a number of Jominy hardenability tests to compare predicted hardenability with measured results. Their comparison indicated that a mid-range composition of the Cr-free steel has a very similar core hardenability profile to a mid-range composition of 8620, and that the case hardenability of the Cr-free steel was only slightly less than that of the 8620. The Cr-free steel composition employed in Phase II had an intentional high side Mn level, pushing the Jominy core hardenability curve to the high side of the SAE 8620H hardenability band. The results obtained were very similar to those expected.

A comparison of the CCT diagrams for 8620 and the Cr-free steels (Figs. 5 and 6) indicates that the transformation characteristics (at the core carbon level) are quite similar. The slight hardenability advantage of the Cr-free steel resulting from the high side Mn level and the fact that faster cooling rates were employed in analyzing the Cr-free steel are both likely reasons for the appearance of the martensite region in the CCT diagram at fast cooling rates. (See Fig. 6.) Because molybdenum has a strong retarding effect on the ferrite plus pearlite (F+P) reaction, the somewhat longer starting times for F + P in the Cr-free steel are probably a result of the increased molybdenum level. In general, the results from Phase I and Phase II indicate that both case and core hardenability of the Cr-free steel are equivalent to 8620.

Carburizing results performed on laboratory specimens indicated that even though the carbon profiles obtained on 8620 and Cr-free steels were similar, the hardness profiles were higher on the Cr-free steel. Retained austenite profiles indicated that this was not due to a difference in the amount of retained austenite between the steels. Since carbon content controls the hardness of the transformed martensite, the fact that the 8620 hardness values were lower near the surface suggests that the Cr in the 8620 may tie up some of the carbon near the surface as carbide. Sharma and Keith[1] observed in the case hardenability tests of Phase I that the surface carbon content after pack carburizing was lower in the Cr-free steel than the 8620. They concluded that, because of the elimination of the Cr, the Cr-free steel had

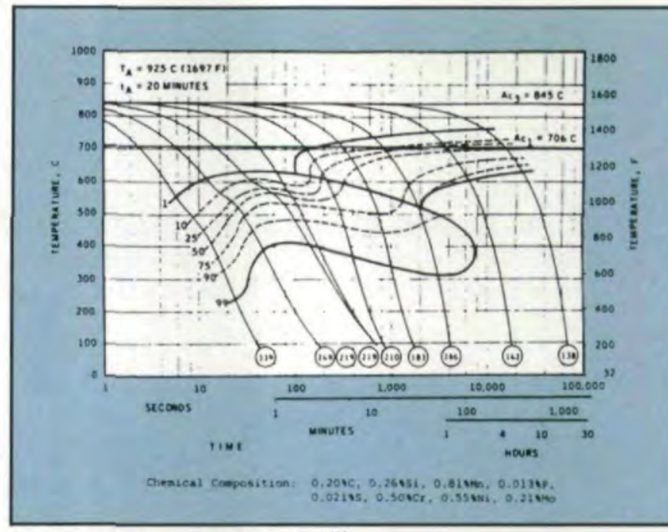

Fig. 5 – CCT diagram for 8620 steel.[3]

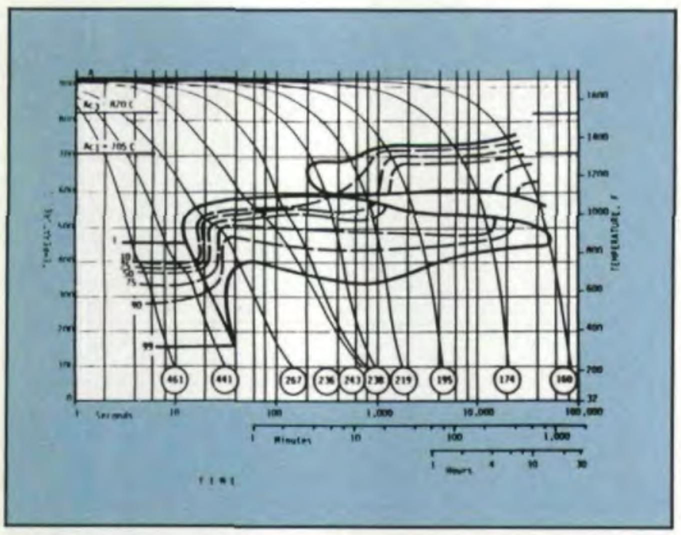

Fig. 6 – CCT diagram for Cr-free steel.

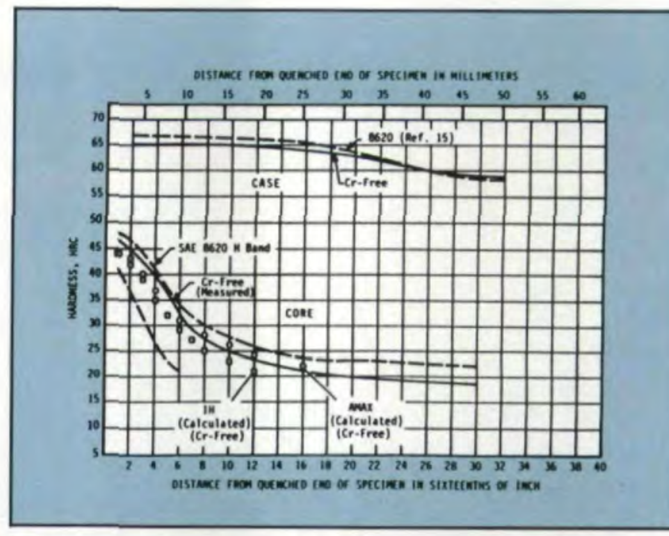

Fig. 7 – Case and core Jominy hardenability test results for Cr-free compared with published data and calculated predictions.

Fig. 8a – 8620 flank surface (unetched) showning IGO penetration (≈ 0.0007). Also shows a cluster of sulphide particles. (400X)

Fig. 8b – (Cr-Free) Flank surface (unetched showing IGO penetration (0.0007).

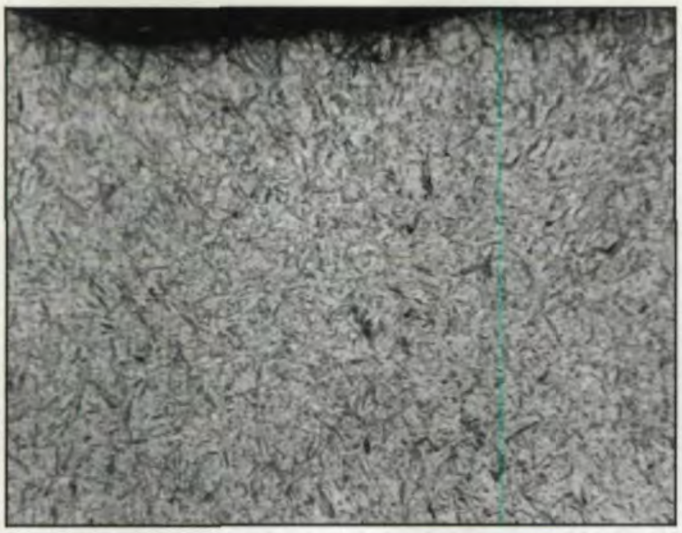

Fig. 9a – Etched 8620 root area surface. Strucure is martensite and austenite. (400X)

Fig. 9b – Cr-free root area surface. Structure is martensite and austenite. (400X)

Fig. 10a – 8620 flank in etched condition. Structure is a martensite austenite mix. (400X)

Fig. 10b – Cr-free flank (etched) to show martensite austenite structure. (400X) a reduced tendency to form carbides and would, therefore, tolerate a greater variation in furnace carbon potential than the 8620.

Hardenability comparisons are shown in Fig. 7. Only the hardenability of the Cr-free steel was measured. The comparison is made with published base (core) and case hardenability for 8620. The hardenabilities of the two steels are comparable in this program.

Microstructure, Grain Size and Cleanliness

These three items are critical to performance. Since in both bending and pitting fatigue, the fracture origins are at or very near the surface, it was critical that the Cr-free steel be capable of developing suitable properties near the surface.

Near surface microstructures are compared in Figs. 8, 9, and 10. In addition to the conventional microstructure, which is intended to be a mix of martensite and austenite, surface intergranular oxidation (IGO) also plays an important role. Figs. 8a and 8b compare the two steels' conditions in the unetched condition. Both show normal penetration of IGO.

Figs. 9a, 9b, 10a and 10b compare their structures in the etched condition. Both are considered acceptable and normal. The 8620 control group seems to have had a slightly greater tendency to form transformation products in the IGO layer, although it is quite moderate. The core structures, not shown, were identical.

X-ray retained austenites were also compared. (Refer to Table 2.) Except for the value at 0.005", the results were almost identical.

TABLE 2

	X-RAY DIFFRACTION RETAINED AUSTENITE Cr-free Alloy	8620H
Surface	20%	22%
0.002	32%	35%
0.005	23%	36%
0.010	27%	27%

Cleanliness, of course, is a result of melting, pouring and rolling practice. Cleanliness was measured on both the raw material (ASTM and SAE methods) and qualitatively on finished parts as a part of the post mortem investigation. Both steels were very clean.

Both steels were made by a fine grain practice. The Cr-free steel contained 0.05 Al, the 8620, 0.03 Al. Grain size measured ASTM #9.5, as shown in Fig. 11. A heat etch method was used. In this method, a polished sample is heated to the test temperature (1700°) in a protective atmosphere. Boundary zones are accentuated (grooved) due to selective vaporization and diffusion.

Grain Flow

Rolled steel products, such as alloy steel bars for forging, have grain flow characteristics that are dependent on how they have been reduced to size. This grain flow is modified by the forging operation.

Figs. 12 and 13 compare the grain flow characteristics of two gears from the program. The 8620H was forged by axially compressing a 2" round cornered square cut to 3⅛" lengths. The

Fig. 11 – Typical prior austenite grain size (heat etch). (100X)

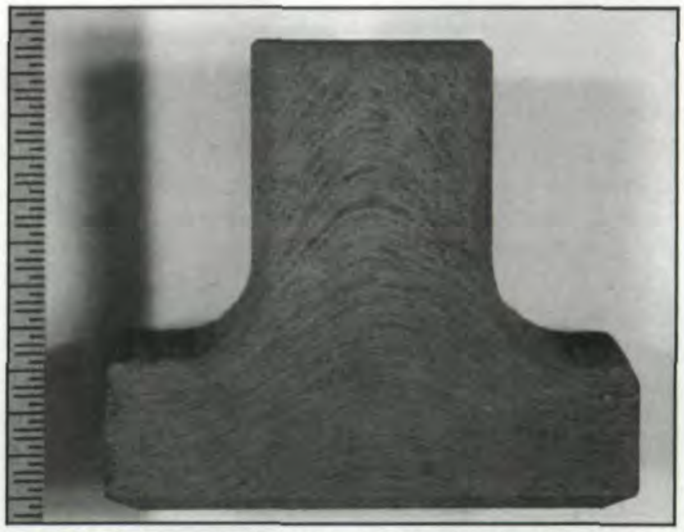

Fig. 12 – Grain flow – Specimen #25 – 8620H etchant: hot HCL. (2.8X)

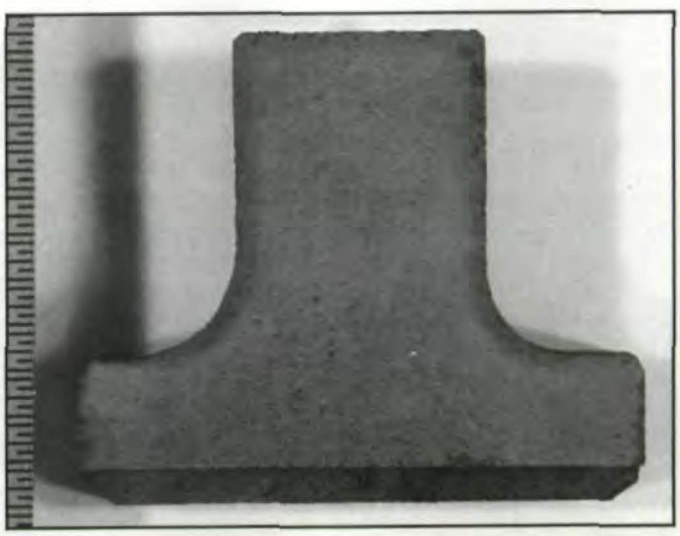

Fig. 13 – Grain flow – Specimen #18 – Cr-free alloy #4 etchant: hot HCL. (3.0X)

Cr-free was forged from a 2⅜" round cornered square cut to 2¼" lengths. The compression direction could have been random, since it was nearly a cube. The views shown are from an axial cross section of a forging from each group to show longitudinal flow lines. The tooth load is applied perpendicular to the photograph. The 8620 shows typical flow lines. Although showing faint typical flow lines, Cr-free also shows significant end grains. The effect of this on performance is not known. It is not necessarily significant, as neither have flow lines which are optimum.

Effect of High Manganese

The maximum Mn level in the Cr-free steel is higher than that generally seen in low alloy steels. Most low alloy steels, except for those in the AISI-SAE 1300 series, have maximum Mn levels of 1.00% or less. Historically, high-side Mn levels have been associated with problems such as alloy segregation during ingot casting leading to banding, as well as intergranular oxide (IGO) formation during carburizing. The Mn level in the 10-ton heat used in this investigation was intentionally held to the high side of the suggested range so that questions such as these could be evaluated.

The extent of Mn segregation is a function of the size of the ingot and the cooling rate; i.e., smaller ingots with faster cooling rates will show less segregation than larger ingots. Although the heat size was small, the single ingot that was cast is roughly similar to what is used commercially. Hence, the cooling rates obtained during solidification were representative of those obtained in commercial ingot practice. Thus, to the extent that this investigation was able to duplicate a commercial practice, there was no indication that the Mn level of the Cr-free steel would produce excessive segregation.

Another concern associated with the Cr-free steel is the extent to which the high Mn level would increase the IGO formation during carburizing. IGO is an unavoidable product of most commercial carburizing processes (except vacuum carburizing) for alloys containing Cr, Mn and Si. Published research[9] indicates that these elements will be depleted from solution and will form oxides in the grain boundaries or in the matrix near the surface. The Si content of the steel grades used in most carburizing applications (approximately 0.25%) appears to be the major factor affecting the formation of IGO. The major detrimental aspect of IGO formation is a reduction of case hardenability due to alloy depletion. Although there has not been a definitive study on the relative contribution of Mn and Cr to IGO formation, the slight increase in Mn level can be expected to be offset by the total elimination of Cr in favor of increased Mo which does not oxidize under carburizing conditions.

A comparison of the micrographs in Figs. 8a and 8b suggests that the IGO formation in the Cr-free steel may even be slightly

Fig. 14 – View showing shape and toughness of root fillet. Specimen #3 – Cr-free alloy 20X.

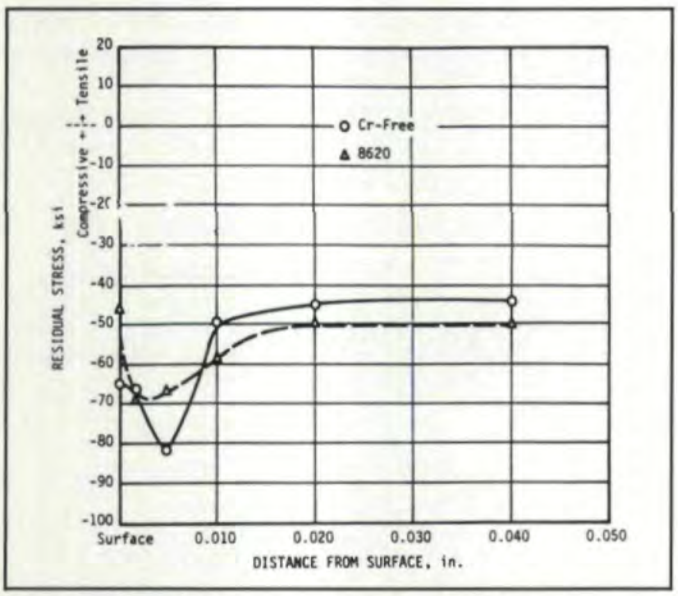

Fig. 15 – Typical residual stress profile shot cleaned like the data base gears.

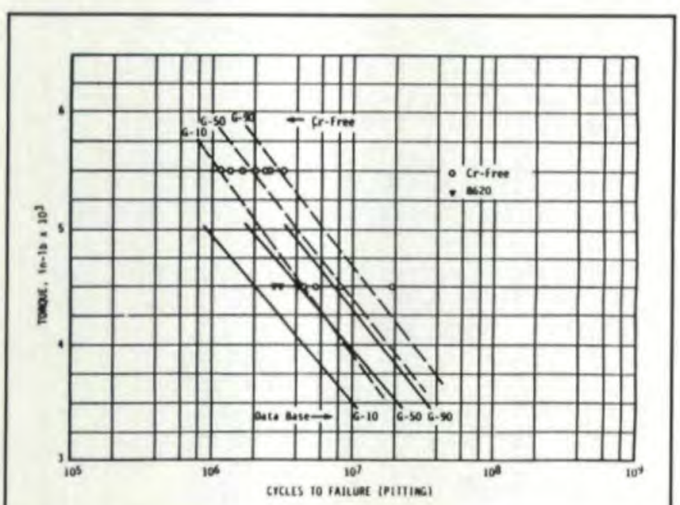

Fig. 16 – Comparison of durability test results of Cr-free and 8620 and data base. Cr-free Weibull distribution is shown along with similar results of the data base.

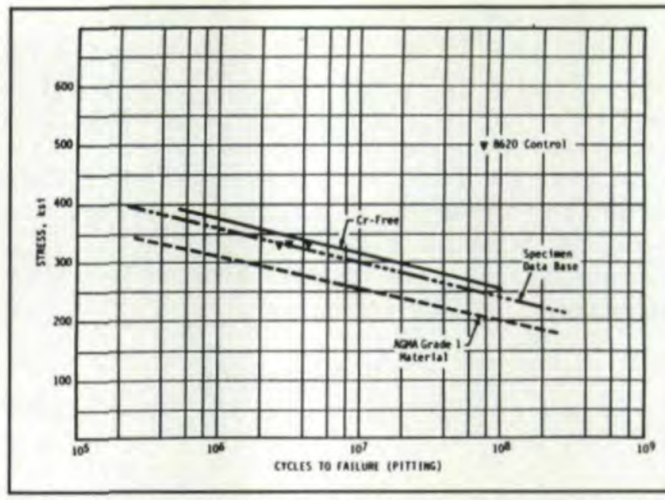

Fig. 17 – Comparison of G-10 Weibull point from durability tests with AGMA allowable stress specificaton for Grade 1 (Reg. 5).

less than that formed in the 8620. The fact that the Cr-free steel performed better than the data base in strength tests may be related to this factor (low IGO formation) also, but unless an analysis is conducted to evaluate relative IGO formation tendencies of the alloys used in the data base, this can only be presented as a possibility. Strength testing will be discussed subsequently.

Dimensioning and Heat Treat Distortion

All gears were processed in a similar manner. The manufacturers reported that the 8620 and the Cr-free materials were similar. Profile, lead checks and "over pin" changes were indistinguishable between the two sets. Both fillet radius and surface finish were basically the same and similar to the "data base" gears. A typical fillet profile is shown in Fig. 14. Surface roughness measured ≈ 125 rms.

Residual Stress

Residual stresses from processing; i.e., heat treat and post heat treat processes, such as cleaning and peening, are known to have major influence on fatigue performance, especially bending fatigue. Some influence is expected in contact fatigue, but less published data is available on this subject.

Variations in residual stress caused an unexpected and unwanted excursion in the test program. The data base is, as noted in Fig. 2, for shot *cleaned* gears. The root fillet compressive residual stress of cleaned gears usually varies from about 40Ksi to 70Ksi The first gear tested in bending (6200 lb-in) gave highly suspect results in that it lived well past the normal failure cycles for bending and then finally failed by pitting. This prompted an investigation of residual stresses. The FASTRESS method was used. Gears from this group were determined to contain a residual stress level of about 87Ksi. This level of residual stress is more in line with shot peened gears. The supplier had done an exceptional job of cleaning the gears. Because of this, it was deemed necessary to replace some of them. The replacement gears were processed through the same cleaning system as the data base gears. Levels more in line with what was expected were obtained. Comparison of results are shown in Table 3. These comparisons are for axial stress since this direction does not require removal of teeth and thus provided a quick answer to the problem.

Subsequently, the residual root stresses of gears from both

TABLE 3 X-Ray Residual Stress Analysis						
		Residual Stress,* ksi				
Identification	Position:	A	B	C	D	Avg.
8620 Cleaned by Supplier		−92	−90	−84	−82	−87
8620 Cleaned Same as Data Base		−44	−40	−58	−34	−44
Cr-Free Cleaned as Data Base		−38	−28	−28	−40	−33.5

*Stress measurements were made at the midpoint of the gear tooth width in the root. They were made at four locations on each gear, 90 degrees apart in the root-axial direction.

groups were characterized in the circumferential direction. An in-depth profile analysis was conducted to determine if there were basic differences. This comparison is shown in Fig. 15. The circumferential direction coincides with the load stress direction and, thus, is a legitimate design consideration.

We elected to use the "over cleaned" gears in the durability (pitting) tests. This aspect will be discussed subsequently.

Power Circulating Gear Tests

Thirty-one gear sets were evaluated, six 8620 and 25 Cr-free. Twenty sets were tested in the durability (pitting) regime and eleven in the tooth strength (breakage) regime. (Refer to Fig. 2.) Tests were split between four load levels, two in each regime. Weibull statistics were used to analyze the data where applicable.

Durability

Figs. 16 and 17 show the torque-cycle results of PC tests conducted in the durability regime in comparison with existing information. The torque levels used were 4500 lb-in and 5500 lb-in. Fig. 16 compares the control group (3 tests) with the data base and the data base with the new Cr-free steel. The 10, 50 and 90% probability levels were determined by analyzing the data for each of the two loads using Weibull statistics.

There are two significant aspects to this data. One, the control group tends to validate the test specimens by falling within the existing data base band. As indicated earlier, these gears were from the "over peened" group. Since both groups — the control group and the test group — were exposed to the same cleaning, it is safe to make comparisons. Two, the Cr-free steel group shows slightly longer lives to pitting than the data base and the control group. In Fig. 17 the 10% probability SN curves of the data base and the Cr-free test group are compared with the G-10 curve for AGMA Grade 1 material. The control group data points are also shown. The AGMA recommended practice is slightly conservative to both the data base and the Cr-free data. This comparison again shows the Cr-free steel to be marginally better than the data base materials. Given the limitations of the analysis in terms of numbers of tests, etc., it is appropriate to conclude that the two groups perform comparably in terms of pitting fatigue.

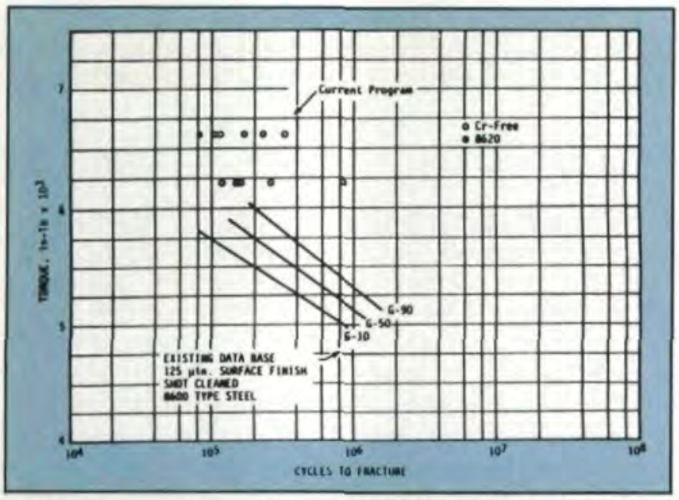

Fig. 18 – Comparison of strength test results of Cr-free and 8620 with data base. Cr-free results are shown with Weibull analysis results of the data base.

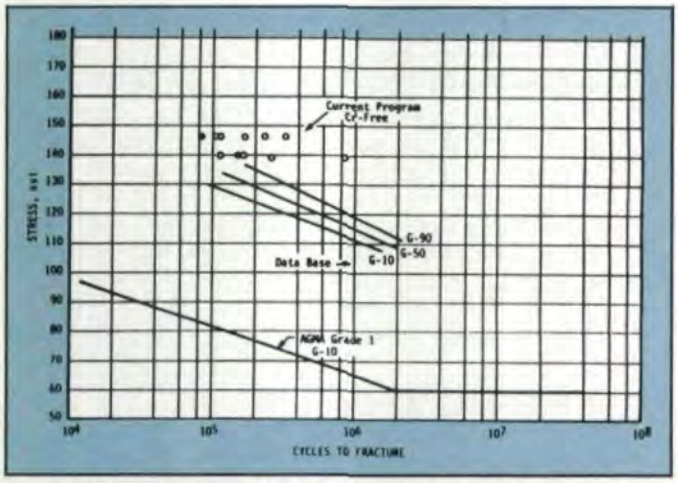

Fig. 19 – Comparison of results from strength tests with data base and the allowable stress specification for AGMA Grade 1.

Tooth Strength

The data generated for comparing bending fatigue is shown in Figs. 18 and 19. The two load levels were 6200 lb-in (139,500 psi) and 6600 lb-in (148500 psi). These load levels are quite close together for this type testing; however, it was necessary to go as high as 6200 lb-in to assure tooth fracture instead of pitting, and the 6600 lb-in is near the upper limit of the test machine being used. Even so, gearing and shaft failures were experienced during this phase of the program.

Fig. 18 shows all data points, including the control group, in comparison with the G-10, 50 and 90 curves for the data base. In one of the tests at 6200 lb-in, the test was terminated due to pitting after 805,000 cycles; i.e., fracture did not occur. There is not quite enough data to perform a legitimate statistical analysis; however, two conclusions can be made. One, the control group samples ran to the low side of the Cr-free group, but to the high side of the data base; and two, the Cr-free group appears to be able to carry higher torques at the same cycles compared to the data base.

Fig. 19 shows this same data, but in terms of stress plotted along with the AGMA allowable stress curves. In this comparison the AGMA design curves appear very conservative. This may be due to many factors, including metallurgical quality, size effects, etc. It is apparent, though, that with good control, gears can be designed and used at significantly higher loads than those indicated.

Summary

1. The Cr-free steel had equivalent (marginally better) durability characteristics compared to the data base.

2. The Cr-free steel exhibited significantly higher strength (tooth bending fatigue) than the data base steel.

A number of factors may be involved, the two most likely being metallurgical quality and residual stress. Since the data base represents a large number of gear sets, it probably included gears with a wider variety of cleanliness, microstructure and residual stress conditions. The Cr-free steel had good structure, was fairly clean and contained residual stress to the high side of that expected for cleaned gears. Thus, this small group may represent high-side performance for these type steels.

3. The hardenability response was pretty much as predicted and, thus, microstructures were satisfactory. This tends to validate the concept of developing substitute steels based on equivalent hardenability. Some reservations are in order as mentioned earlier.

4. Processing characteristics, from steel melting to rolling to forging to machining to heat treating for the Cr-free steel, were similar to other alloy steels of the 8620 type.

5. It was not necessary to modify the green size from that customarily employed in order to accommodate the Cr-free steel movement in heat treatment.

6. Grain flow was different in the Cr-free gears as compared to the control group and the data base gears. This difference is not thought to be of great significance, however, more work is required to validate this assumption.

Conclusion

The purpose of this investigation was to provide a performance comparison between the proposed Cr-free steel composition and the current AISI-SAE 8620 steel grade. None of the comparative tests indicated a compromise in properties as a result of the substitution of Cr-free steel for 8620. On the contrary, there were several points in favor of the substitution. Phase II of this research has built upon the results obtained in Phase I by evaluating the Mn-Mo Cr-free 8620 steel substitute proposed in Phase I in a scaled up application. This Cr-free steel composition was cast as a 10-ton heat and evaluated in a carburized gearing test program along with an 8620 steel control group of gears. The control group was used to calibrate an existing data base with which the new steel was compared. A variety of production, performance and metallurgical aspects of the Cr-free steel were compared with the characteristics of 8620 in an effort to determine whether the Cr-free steel could be recommended as a suitable alternate composition for 8620 in the event of an interruption of the domestic chromium supply. The major conclusions obtained from this program can be summarized as follows:

1. The performance of the Cr-free steel in a carburized gearing test program was at least equivalent to or slightly better than the performance obtained in a similarly processed 8620 control group. In addition, the Cr-free steel performance in the gearing test fell to the high side of an existing data base obtained from steels of similar hardenability. These test results indicated that the Cr-free steel would perform at least as well as 8620.

2. The various processing characteristics that were evaluated indicated that the Cr-free steel could easily be substituted for 8620 steel in existing application with little or no processing changes. For instance, in the production of the gears in this investigation, no significant differences were observed between the Cr-free and 8620 steels in forging, machining or heat treatment.

3. Detailed metallurgical evaluation of the Cr-free and 8620 steels indicated that transformation characteristics, microstructures and fracture morphologies were similar, that no segregation problems were encountered with the higher Mn level of the Cr-free steel and that both steels had similar core and case hardenability.

4. The overall performance of the Cr-free steel is sufficiently similar to that of 8620 that direct substitution of the Cr-free steel for 8620 can be made in gearing applications with no loss in performance characteristics and with little or no change in processing parameters. In other general structural applications, it is expected that the Cr-free steel will process and perform in a similar manner to 8620 steel.

This work has significantly added to the knowledge base required to make successful substitutions in critical applications. It further proved the metallurgical design system for substitution and encourages its use for peaceful purposes, such as cost control.

References

1. SHARMA, V.K. and KEITH, C.J. "Development of Chromium-Free Grades of Constructional Alloy Steels." Report Under Contract #J0113104 of the U.S. Bureau of Mines, 1983.
2. BREEN, D.H., et al. "Computer-Based System Selects Optimum Cost Steels," Parts I – V, ASM Metals Progress starting December, 1972, Metals Park, OH.
3. CAMERON, T.B. "Production and Testing of a Chromium-Free Heat Treatable Alloy Steel." Report Under Contract #J0145009 of the U.S. Bureau of Mines, 1986.
4. BREEN, D.H. "Fundamentals of Gear Stress/Strength Relationship – Materials," SAE SP-584, Paper #841083, September, 1984.
5. AGMA Standard 218.01, American Gear Manufacturers Association, Arlington, VA.
6. SHARMA, V.K., WALTER, G.H., and BREEN, D.H. "An Analytical Approach for Establishing Case Depth Requirement in Carburized Gears." ASME Technical Paper #77-DET-152.
7. IBID. 2, Part III, April, 1973.
8. Atlas: Hardenability of Carburized Steels, Climax Molybdenum Co., 1960, P. 82.
9. CHATTERJEE-FISCHER, R. "Internal Oxidation During Carburizing and Heat Treating." Met. Trans. 9A, Nov., 1978, pp. 1553-60.

Acknowledgements: *Funding for the research outlined above was provided by the U.S. Bureau of Mines. The program was a joint venture of AMAX Materials Research Center, Ann Arbor, MI, and ASME Gear Research Institute, Naperville, IL.*

Reprinted with permission of the American Gear Manufacturers Association. The opinions, statements and conclusions presented in this paper are those of the authors and in no way represent the position or opinion of the AMERICAN GEAR MANUFACTURERS ASSOCIATION.

CIMA USA YOUR SOURCE FOR WORLD CLASS GEARMAKING TECHNOLOGY...

... lets you select familiar component systems

Gear Span Measurement – An Analytical Approach

Ilya Bass
Bourn & Koch Machine Tool Co.
Rockford, IL

The interrelation between span measurement M_s and normal circular tooth thickness T_n can be found by the following formula: (See Fig. 1.)

$$M_s = D_b \cdot \omega$$

$$\omega = \frac{(0.5Dp \cdot inv\phi n) \cdot 2 + Zs \cdot Pnc - Pnc + Tn}{D_p}$$

or, after substituting P_{nc} by $\frac{\pi}{P_{nd}}$ and $\frac{D_b}{D_p}$ by $\cos \phi_n$

$$M_s = \left(\frac{Z}{P_{nd}} \cdot inv\phi_n + \frac{\pi \cdot Zs}{P_{nd}} - \frac{\pi}{P_{nd}} + T_n\right) \cos\phi_n. \quad (1)$$

where

P_{nd} = normal diametral pitch
P_{nc} = normal circular pitch
ϕ_n = normal pressure angle
Z = number of teeth in gear
Z_s = number of teeth spanned
D_p = pitch diameter
D_b = base diameter.

The formula (Equation 1) by itself is not difficult to work with; nevertheless, as soon as one tries to use it, a question arises: What number of teeth spanned should be used? The most common approach employs empirical formulae, tables or diagrams. In most cases, this approach provides satisfactory results, but has two drawbacks. First, it does not assure correct results for nonstandard gears and, secondly, the tables and diagrams are not very convenient for computerization.

The purpose of this article is to describe an analytical method free of the drawbacks mentioned above and providing absolutely reliable results.

Equation 1 can be rearranged to express the number of spanned teeth:

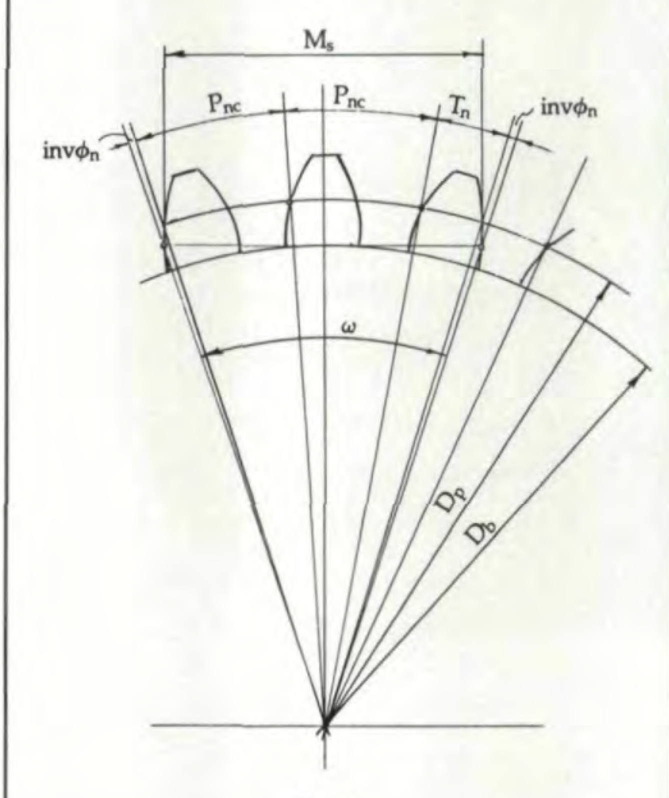

Fig. 1

$$Z_s = \frac{Pnd \cdot Ms}{\pi \cdot \cos\phi_n} - \frac{Z}{\pi} \cdot inv\phi_n - \frac{Pnd \cdot Tn}{\pi} + 1 \quad (2)$$

Assume *a priori* that Z_s has restrictions on its minimum and maximum values; i.e.,

$$Z_{smin} < Z_s < Z_{smax} \quad (3)$$

Now we must determine whether these restrictions exist and, if they do, how they can be determined.

As follows from Fig. 2, the measurement line A-A_1 is tangent to the base diameter D_b and perpendicular to axis Y. The line intersects the different teeth of the gear and, according to geometrical properties of the involute curve, is always normal to the tooth profile. This, in turn, means that the amount of outside diameter D_o can be considered as a theoretical

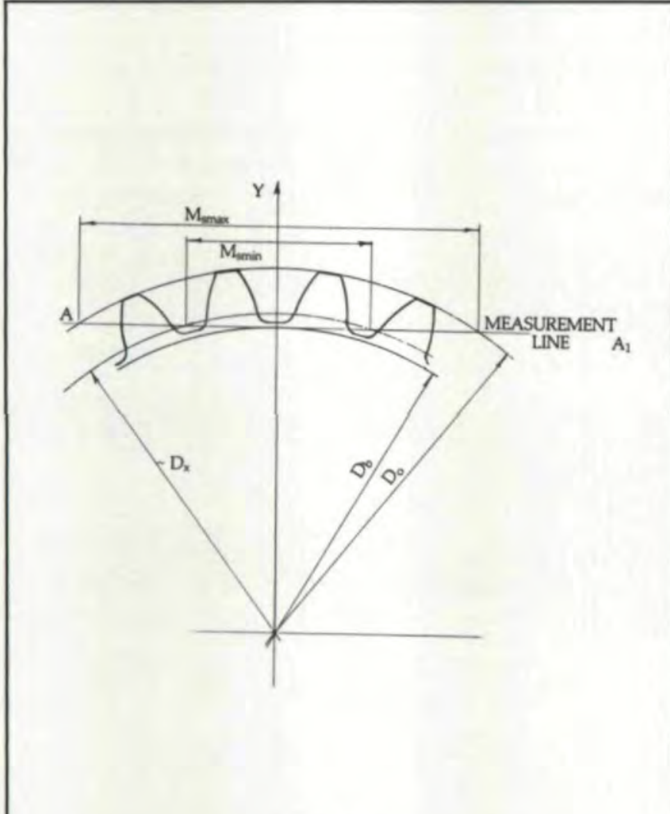

Fig. 2

restriction for the maximum allowable amount of span measurement:

$$M_{smax} = \sqrt{D_o^2 - D_b^2}$$

Therefore,

$$Z_{smax} = \frac{Pnd \cdot Msmax}{\pi \cdot \cos\phi_n} - \frac{Z}{\pi} \cdot inv\phi_n - \frac{Pnd \cdot Tn}{\pi} + 1 \quad (4)$$

For gears with tip relief or other tip modification, D_o should be replaced with the corresponding diameter. From the practical standpoint, the amount of M_{smax}, calculated by Equation 4, should be reduced.

The minimum acceptable number of spanned teeth must be chosen on the condition that the contact diameter should always be located above the true involute form (TIF) diameter D_x. Otherwise, the measurement itself will be taken on the fillet rather than on the involute form of the tooth profile. Therefore,

$$M_{smin} = \sqrt{D_x^2 - D_b^2}$$

$$Z_{smin} = \frac{Pnd \cdot Msmin}{\pi \cdot \cos\phi_n} - \frac{Z}{\pi} \cdot inv\phi_n - \frac{Pnd \cdot Tn}{\pi} + 1 \quad (5)$$

As with every similar algebraic expression, the expression (3) may have many solutions, one solution or no solution at all. The last two results might occur in the case of nonstandard gears with a small number of teeth. Of course, one tooth "spanned" is always possible, but we do not consider it as spanned.

Thus, to provide a correct approach to span measurement calculations, the true involute form diameter must be known. Unfortunately, many gear manufacturers have to deal with the blueprints where the TIF diameter is not indicated. In this case, it is a good policy to determine the number of spanned teeth by taking the contact diameter as close as possible to the pitch diameter.

The formula for calculating Z_s can be derived by the following steps.

Without losing much accuracy, the T_n can be replaced by $\frac{Pnc}{2}$ since $P_{nc} = \frac{\pi}{Pnd}$. Equation 2 can be rewritten as

$$Z_s = \frac{Ms \cdot Pnd}{\cos\phi_n \cdot \pi} - \frac{Z}{\pi} \cdot inv\phi_n + 0.5 \quad (6)$$

Since the contact diameter was assumed to be equal to the pitch diameter, the following expression is true:

$$M_s = D_p \cdot \sin\phi_n = \frac{Z}{P_{nd}} \cdot \sin\phi_n$$

Substituting the value of M_s from this equation into (6) we receive:

$$Z_s = \frac{Z}{\pi} \cdot \tan\phi_n - \frac{Z}{\pi} \cdot inv\,\phi_n + 0.5 \quad (7)$$

After simplifying (7) the final result is:

$$Z_s = \frac{Z}{\pi} \cdot \phi_n + 0.5 \qquad (8)$$

This formula has been successfully applied to gears with standard addenda and dedenda and, very often, to non-standard gears. For non-standard gears, additional checking needs to be done.

Below are numerical values for the most common pressure angles (spur gears):

$$Z_s = \frac{Z}{12.4} + 0.5 \quad \text{for } \phi_n = 14.5°;$$

$$Z_s = \frac{Z}{9} + 0.5 \quad \text{for } \phi_n = 20°;$$

$$Z_s = \frac{Z}{7.2} + 0.5 \quad \text{for } \phi_n = 25°.$$

The rounded Z_s must satisfy the conditions found in Equation 3 and then be used in (1), the final form of which can be arranged more conveniently for computing purposes:

$$M_s = [T_n \cdot P_{nd} + Z \cdot \mathrm{inv}\phi_n + \pi(Z_s - 1)] \frac{\cos\phi_n}{P_{nd}}$$

The program developed on the given approach calculates span measurement for both cases – with and without TIF diameter. When TIF diameter is entered, the program prints out a set of all possible solutions in accordance with the restrictions in Equation 3. The final choice is up to the manufacturer and should be based on his ability to manufacture certain sizes, the rigidity of the caliper, etc.

The formulae given in this article are easily adjustable for helical gears. It is sufficient to replace dimensions in the normal plane by those in the transverse one. For example, the last formula can be rewritten as

$$\frac{Ms}{\cos\psi_b} = [T_n \cdot P_{nd} + Z \cdot \mathrm{inv}\phi + \pi(Z_s - 1)] \frac{\cos\phi}{P_{nd} \cdot \cos\psi}$$

Since

$$\cos\phi = \frac{\cos\phi_n \cdot \cos\psi}{\cos\psi_b}$$

After substituting and simplifying, it will acquire the following form:

$$M_s = [T_n \cdot P_{nd} + Z \cdot \mathrm{inv}\phi + \pi(Z_s - 1)] \frac{\cos\phi_n}{P_{nd}}$$

For helical gears one additional restriction on the number of spanned teeth should be considered. Gear hobbing width must be more than M_s * $\sin\psi_b$, where ψ_b – the base helix angle.

Example Calculation for Helical Gears

A helical gear has the following data:
$Z = 19$, $P_{nd} = 8$, $\phi_n = 14.5°$, $\psi = 27°16'$, $D_o = 2.922$, $D_x = 2.645$, $T_n = 0.1962$, gear face width $= 1.25$.

Transverse pressure angle ϕ:

$$\tan\phi = \frac{\tan 14.5°}{\cos 27.266667°}; \qquad \phi = 16.222165°$$

Involute of ϕ:

$$\mathrm{inv}\phi = 0.007816$$

Pitch Diameter D_p:

$$D_p = \frac{19}{8 \cdot \cos 27.266667^\circ} = 2.67189$$

Base Diameter D_b:

$$D_b = 2.67189 \cdot \cos 16.222165^\circ = 2.56551$$

Base Helix angle ψ_b:

$$\sin\psi_b = \sin 27.266667^\circ \cdot \cos 14.5^\circ;\ \psi_b = 26.32996^\circ$$

Maximum Span Measurement M_{smax}:

$$M_{smax} = \sqrt{2.922^2 - 2.56551^2} \cdot \cos 26.32996^\circ$$

$$M_{smax} = 1.253553$$

Minimum Span Measurement M_{smin}:

$$M_{smin} = \sqrt{2.645^2 - 2.56551^2} \cdot \cos 26.32996^\circ$$

$$M_{smin} = .576803$$

Number of Z_{smax}:

$$Z_{smax} = \frac{8 \cdot 1.253553}{\pi \cdot \cos 14.5^\circ} - \frac{19}{\pi} \cdot 0.007816 - \frac{8 \cdot 0.1962}{\pi} + 1$$

$$Z_{smax} = 3.75$$

Number of Z_{smin}:

$$Z_s\text{min} = \frac{8 \cdot 0.576803}{\pi \cdot \cos 14.5} - \frac{19}{\pi} \cdot 0.007816 - \frac{8 \cdot 0.1962}{\pi} + 1;$$

$$Z_{smin} = 1.97$$

Accepted number of spanned teeth:

$$Z_s = 3$$

Span measurements M_s:

$$M_s = [0.1962 \cdot 8 + 19 \cdot 0.007816 + \pi(3-1)] \frac{\cos 14.5^\circ}{8}$$

$$M_s = 0.9683$$

Checking for gear width:

$$0.9683 \cdot \sin 26.32996^\circ = 0.43$$

AUTHOR:

For 25 years, **ILYA BASS** *has been involved in practical and research work relating to manufacturing systems and cutting tools. He has authored two books and numerous articles on gear cutting tools. Currently, Bass is a Programmer/Software Engineer at Bourne & Koch Machine Tool Co. in Rockford, IL. He is also a senior member of SME.*

Into-Mesh Lubrication of Spur Gears — Part I

L. S. Akin
Gearesearch, Inc.
Banning, CA
and
D. P. Townsend
NASA Lewis Research Center
Cleveland, Ohio

Abstract:

An analysis was conducted for into-mesh oil jet lubrication with an arbitrary offset and inclination angle from the pitch point for the case where the oil jet velocity is equal to or less than pitch line velocity. The analysis includes the case for the oil jet offset from the pitch point in the direction of the pinion, and where the oil jet is inclined to intersect the common pitch point. Equations were developed for the minimum oil jet velocity required to impinge on the pinion or gear and the optimum oil jet velocity to obtain the maximum impingment depth.

The optimum operating condition for best lubrication and cooling is provided when the oil jet velocity is equal to the gear pitch line velocity with both sides of the gear tooth cooled. When the jet velocity is reduced from pitch line velocity, the drive side of the pinion and the unloaded side of the gear is cooled. When the jet velocity is much lower than the pitch line velocity the impingement depth is very small and may completely miss the pinion.

Introduction

Several methods of oil jet lubrication of gears are practiced by the gear industry. These include the oil jet directed into the mesh, out of the mesh and radially directed into the gear teeth. In most cases an exact analysis is not used to determine the optimum condition such as, jet nozzle location, direction and oil jet velocity, for best cooling. As a result many gear sets are operating without optimum oil jet lubrication and cooling.

The reason for developing more precise gear lubrication and cooling analysis is to provide more design control over the scoring mode of gear tooth failure.[1-4] As a result, considerably more power capacity can be provided in smaller gear drives. This is especially crucial in high performance aircraft or aerospace and light weight marine gears where the gears are case-hardened and ground.

The first step in performing such an analysis is to determine the oil jet impingement depth down the tooth profile being cooled by the jet. The radial and out-of-mesh jet nozzle orientation analyses have already been published.[2, 3] The analysis discussed in this paper is confined exclusively to the directly into-mesh jet nozzle orientation where oil jet velocity is less than or equal to the gear pitch line velocity ($V_j \leqslant \omega R \sec \beta_p$).

Primary impingment *only* is considered here because it can be accurately controlled. If it is properly applied, primary impingement alone can provide nearly all the necessary cooling. Post-impingement flow down the tooth profile is not considered in this analysis. This nozzle orientation is the least desirable from a cooling viewpoint in that the fling-off angle and fling-off time[5] are severely curtailed because the immediate tooth engagement drastically reduces the lubricant residence time and the effective heat transfer.

The time when this orientation is desirable is (a) when the speed is so slow as to provide inadequate elasto-hydrodynamic (EHD) lubricant film thickness in the mesh conjunction zone, increasing the coefficient of friction and heat generation, and (b) when the speed is so high that radial or out-of-mesh impingement allows the fling-off angle and time to be so small as to provide inlet or EHD entrance zone film starvation.

Thus, in this case the problem is not cooling, but one of lubricant supply in the conjunction zone. In such cases, multiple nozzle orientation may be desirable: one very small into-mesh jet for lubrication and one or more larger out-of-mesh jets for cooling.

The objective of the work reported herein was to develop the analytical methods for gear lubrication with the oil jet directed into the engaging side of the gear mesh. The analysis when the oil jet velocity is less than pitch line velocity differs considerably from the case when it is greater than pitch line velocity; therefore, this paper deals only with the case of oil jet velocity equal to or less than pitch line velocity. At gear ratios larger

AUTHORS:

DR. LEE S. AKIN *has been working in mechanical engineering since 1947, specializing principally in technologies related to rotating machinery. About half of this time has been spent in the gear industry and the other half in the aerospace industry, concentrating on mechanisms involving gears and bearings as well as friction, wear, and lubrication technologies.*

Since 1965, when he received his Ph.D. in mechanical engineering, he has been extensively involved in gear research especially related to the scoring phenomena of gear tooth failure. In 1971 he joined forces with Mr. Dennis Townsend of NASA Lewis Research Center, and together they have produced numerous papers on technologies related to gear scoring. Since 1986, Dr. Akin has been working as a gear consultant with his own company, Gearesearch Inc.

MR. D.P. TOWNSEND *is a gear consultant for NASA and numerous industrial companies. Townsend earned a BSME from the University of West Virginia. During his career at NASA he has authored over fifty papers in the gear and bearing research area. For the past several years, he has served in active committee roles for ASME. Presently he is a member of the ASME Design Engineering Executive Committee.*

than one, the oil jet should be offset from the pitch line and rotated to a precise location to get optimum oil jet impingement on both the gear and pinion.

Analysis

The analyses presented herein used an arbitrary offset and angle for jet location. For best results the offset should be constrained within $0 \leqslant S \leqslant S_o$, where:

$$S_o = a\,\frac{M_g - 1}{M_g + 1}$$

and the impingement angle β should be constrained within $0 \leqslant \beta \leqslant \beta_{pp}$, where:

$$\beta_{pp} = \tan^{-1} \frac{S_o}{(R_o^2 - R_s^2)^{1/2}}$$

In this analysis β will be further constrained so that:

$$\beta_p = \tan^{-1}[(S/(R_o^2 - R_s^2)^{1/2}]$$

so that S is an independent variable and β_p is a dependent variable.

The analyses that follow are divided into two cases (or operational conditions) with subcases. The two cases are determined by whether or not the resolved pitch line velocity in the direction of the cooling oil jet ($V_p = \omega_p r \sec \beta_p = \omega_g R \sec \beta_p$) is equal to or less than the oil jet velocity. Only these two cases are considered in this paper. Also, starting with a unit gear ratio $m_g = 1$ as a reference, consider that the ratio is increased ($m_g > 1$) until the jet is gear-tooth controlled, thus, severely narrowing the operating jet velocity range that will wet the pinion tooth (that is, avoid missing it entirely). This analysis has been broadened in scope from previous published analysis,[6] by allowing an arbitrary offset distance S and a constrained inclination angle β_p. It is assumed that optimum conditions occur if $S = S_o$ and $\beta_p = \beta_{pp}$, removing the V_j (max) and V_j(min) limitations to be described later in the paper.

NOMENCLATURE

a	$1/P_d$ or $(1 \pm \Delta N/2)/P_d$ = addendum
b_p, b_g	pinion and gear backlash respectively
B_p, B_g	total, pinion, gear backlash at $P_d = 1$
d_p, d_g	radial impingement depth
L_p, L_g	pinion, gear final impingement distance
L_{ig}	intermediate impingement distance
m_g	$N_g/N_p = R/r = \omega_p/\omega_G$ = gear ratio
N_p, N_g	number of teeth in pinion, gear
ΔN	differential number of teeth
P_d	diametral pitch
r, R	pinion and gear pitch radii
r_α, R_α	perpendicular distance from pinion, gear center to jet line
r_s, R_s	distance along line of centers to jet line origin
r_x, R_x	distance along line of centers to jet line intersection at x
r_o, R_o	pinion and gear outside circle diameter
r_b, R_b	pinion and gear base radii
S, S_o, S_p	arbitrary, jet nozzle offset to interesect O.D.'s offset for pinion only
t	time
t_f, t_ω	time of flight, rotation
$V_p = V_g$	linear velocity of pinion and gear at pitch line
V_j, V_{jp}	oil jet velocity, general, pinion controlled
x	distance for offset perpendicular to jet line intersection
$V_j(max)_p$	maximum velocity at which $d_p = 0$
$V_j(min)_p$	minimum velocity at which $d_p = 0$
β	arbitrary oil jet inclination angle
β_p	constrained inclination angle
β_{pp}	inclination angle for pitch point intersection
φ	pressure angle at pitch circles
φ_{pi}, φ_{gi}	pinion and gear pressure angle at points specified at i
ω_p, ω_g	pinion and gear angular velocities
inv φ	$\tan\varphi - \varphi$ = involute function at pitch point or operating pressure angle
$V_j(Opt, L)_p$	lower limit jet velocity to impingement at pitch line

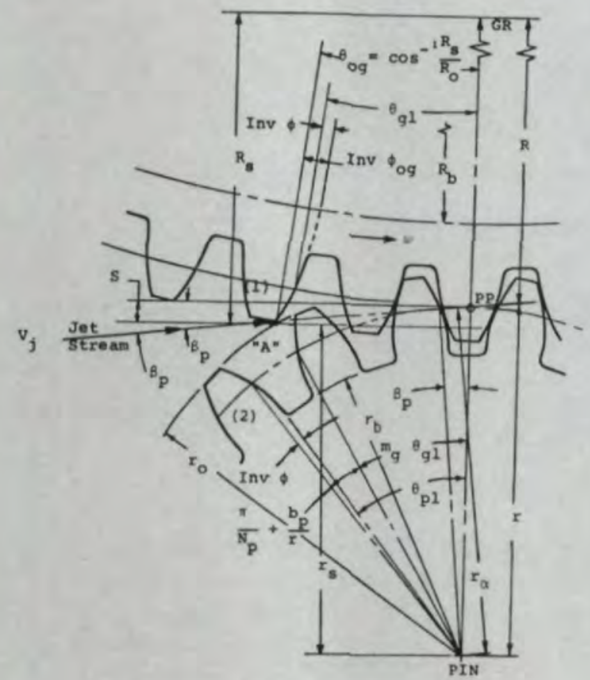

Fig. 1

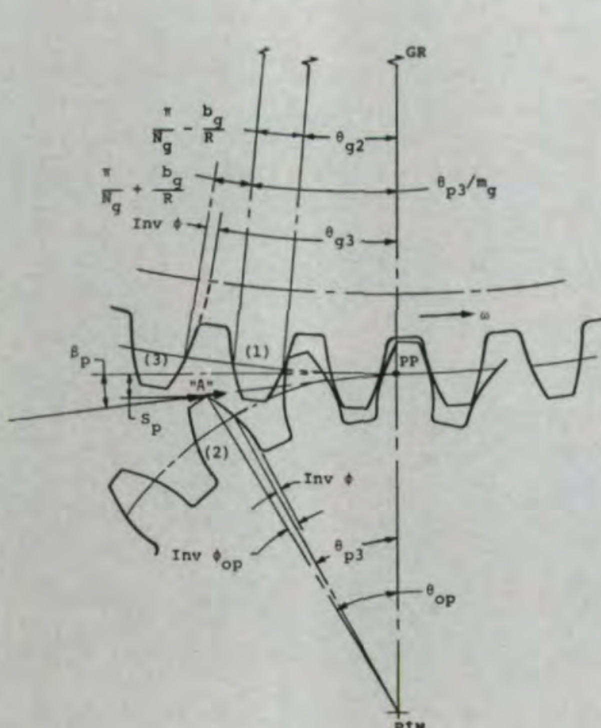

Fig. 2

It becomes overwhelmingly clear as the analysis proceeds that it is desirable to provide an optimum engaging jet velocity exactly equal to or slightly larger than the resolved pitch line velocity, $V_j = \omega_p r \sec\beta_p = \omega_g R \sec\beta_p$, to provide maximum addendum impingement surface area down to the pitch circle on both gear and pinion as pointed out by Fujita et al. in 1965.[7, 8]

Development of Primary Formulae for the Generalized Pinion Cases ($0 \leqslant S \leqslant S_o$)

Assume that we begin to view the sequence of events for the case in which the jet stream velocity $V_j < \omega_p r \sec \omega_p$ (where $\omega_p r$ is the pitch line velocity). (See Figs. 1-3.) As can be seen, the jet stream head initiated by gear tooth (1) at "A" in Fig. 1 will impinge on the leading side of the pinion tooth (2), which is trailing gear tooth (1) in Fig. 2. The so-called impingement depth will be determined by the final impingement of the jet stream head as shown in Fig. 3 at "A". The starting positions of the mating teeth (1) and (2) as shown in Fig. 1 are calculated for the gear:

$$\theta_{gl} = \cos^{-1}(R_s/R_o) - \text{inv}\,\varphi_{og} + \text{inv}\,\varphi \tag{1}$$

where:

$$\text{inv}\,\varphi_{og} = \tan\varphi_{og} - \varphi_{og} \quad \text{and}$$

$$\varphi_{og} = \cos^{-1}(R_b/R_o) = \cos^{-1}[(N_g \cos\varphi)/(N_g + 2 \pm \Delta N)] \tag{2}$$

$$\text{inv}\,\varphi = \tan\varphi - \varphi$$

φ = Pressure angle of gear (or pinion) at pitch circle
R_s = $R + S$ and $r_s = r - S_p$ (See Figs. 1 or 4)
S = Jet offset, $0 \leqslant S \leqslant S_o$ and $S = S_p$ only when $\beta_p = \beta_{pp}$
S_p = $[(r_0^2 - r^2\cos^2\beta_p)^{1/2} + r\sin\beta_p]\sin\beta_p$, $0 < S_p < S$
S_o = Offset that places jet stream at intersection of O.D.'s (crotch)
R = Pitch radius of gear = $N_g/(2\,P_d)$
R_o = Outside radius of gear = $(N_g + 2 \pm \Delta N)/2\,P_d)$
R_b = $R\cos\varphi$ = base radius of gear
$(R_s/R_o) = N_g/(N_g + 2 \pm \Delta N) = m_g N_p/(m_g N_p + 2 \pm \Delta N)$
m_g = Gear ratio = $N_g/N_p = R/r = \omega_p/\omega_g$
N_g = Number of teeth in gear circle
ΔN = Delta (or differential) number of teeth when long and short addendums are used (ΔN is usually set to zero)
P_d = Diametral pitch

Assume $0 \leqslant S \leqslant S_o$ in this paper, unless otherwise stated.
For the pinion:

$$\theta_{p1} = m_g\theta_{g1} + \pi/N_p - \text{inv}\,\varphi + 2\,B_p/N_p \tag{3}$$

where:

N_p = Number of teeth in the pinion circle
B_p = Blacklash at $P_d = 1$, for pinion only
b_p = B_p/P_d = Blacklash at diametral pitch used
(b_p and b_g are usually set equal to zero in these calculations.)

This locates the pinion tooth to be impinged upon by the short jet stream shown in Fig. 2, at time equal to 0 ($t = 0$) in Fig. 1, when its initial end (called "head") reaches the final impingement point "A", (shown in Fig. 3 as impingement length, L_p, and impingement depth d_p). The position of the pinion tooth (2) in Fig. 3 when at $t = t_\omega$ the oil jet head makes this final piont "A" is calculated from:

$$\theta_{p2} = \tan^{-1}\left(\frac{L_p \cos\beta_p}{r - L_p \sin\beta_p}\right) - \operatorname{inv}\varphi_{p2} \tag{4}$$

where:

$$\operatorname{inv}\varphi_{p2} = \tan\varphi_{p2} - \varphi_{p2}$$

$$\varphi_{p2} = \cos^{-1}\left(\frac{r_b}{[(r - L_p \sin\beta_p)^2 + (L_p \cos\beta_p)^2]^{1/2}}\right) \tag{5}$$

β = Inclination angle of jet stream ($0 < \beta < \beta_{pp}$)
β_p = Inclination angle pointing at pitch point (PP), $0 < S < S_o$
$\beta_p = \tan^{-1}[S/(R_o^2 - R_s^2)^{1/2}]$
β_{pp} = Inclination angle pointing at pitch point when $S = S_o$ only
$\beta_{pp} = \tan^{-1}[S_o/(R_o^2 - R_s^2)^{1/2}]$

r = Pitch radius of pinion $= N_p/(2\,P_d)$
$r_b = r\cos\varphi$ = Base radius of pinion

The *design* solution to the problem of pinion cooling is to set the desired impingement depth "d_p" for the needed cooling surface and solve explicitly for the needed jet velocity V_j. It is assumed that $\beta = \beta_p$ in this paper to simplify the mathematics. Noting that the time of jet stream flight t_f must be equal to the time of rotation t_ω, it can be shown that the required jet velocity may be calculated from

$$V_j = \omega_p \frac{[(R_o^2 - R_s^2)^{1/2} \sec\beta - L_p]}{(\theta_{p1} - \theta_{p2})} = V_{jp} \tag{6}$$

where:

$$L_p = [(r_o - d_p)^2 - r^2\cos^2\beta_p]^{1/2} + r\sin\beta_p \tag{7}$$

$$r_o = \text{Outside radius of pinion} = (N_p + 2 \pm \Delta N)/2\,P_d$$

The *analysis* solution to the problem, when V_j is specified and the resulting impingement depth d_p is desired for the pinion, can be calculated implicitly by solving iteratively for $_p$ from:

$$\omega_p[(R_o^2 - R_s^2)^{1/2} \sec\beta_p - L_p] = (\theta_{p1} - \theta_{p2})V_j \tag{8}$$

then

$$d_p = r_o - [(r - L_p\sin\beta_p)^2 + (L_p\cos\beta_p)^2]^{1/2} \tag{9}$$

$$\text{for } 0 < V_j < V_j(\text{Opt}, L)_p$$

and

$$d_p = a = \frac{1 \pm \Delta N/2}{P_d} \tag{10}$$

$$\text{for } V_j(\text{Opt}, L)_p \leqslant V_j$$

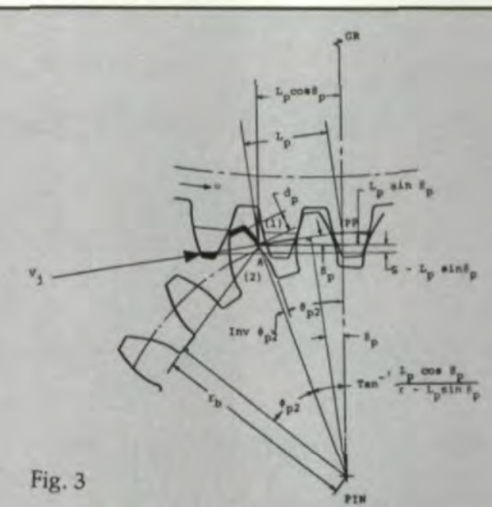

Fig. 3

TABLE 1. - EQUATIONS FOR OIL JET VELOCITY AND PINION IMPINGEMENT DEPTH FOR PITCH LINE AND LOWER OIL JET VELOCITY

Relative velocity scale	Oil jet velocity	Pinion impingement depth
Pitch line and slightly lower	$V_j = \omega_p r \sec \beta_p = \omega_g R \sec \beta_p$ $V_j(\text{opt}, L)_p = \frac{\omega_g (R_o^2 - R_s^2)^{1/2} \sec \beta_p}{\theta_{g1} + \pi/N_g + 2B_g/N_g}$	$d_p = a = (1 \pm \Delta N_p/2)/P_d$, (both profiles) $d_p(\text{head}) = a$, (leading profile only)
Less than pitch line velocity down to where the oil jet starts to miss the pinion	$V_j = \frac{\omega_p [(R_o^2 - R_s^2)^{1/2} \sec \beta_p - L_p]}{\theta_{p1} - \theta_{p2}}$ V_j = given (when $0 \leq d_p \leq a$ only)	d_p = given (usual design solution) and $L_p = [(r_o - d_p)^2 - (r \cos \beta_p)^2]^{1/2} + r \sin \beta_p$ Iterate L_p from $[(R_o^2 - R_s^2)^{1/2} \sec \beta_p - L_p]\omega_p = (\theta_{p1} - \theta_{p2})V_j$ then, $d_p = r_o - [(r - L_p \sin \beta_p)^2 + (L_p \cos \beta_p)^2]^{1/2}$
Critical low velocity to miss the pinion	$V_j(\min)_p = \frac{\omega_p[(R_o^2 - R_s^2)^{1/2} \sec \beta_p - (r_o^2 - r_s^2)^{1/2} \sec \beta_p]}{\theta_{p1} - \theta_{p3} + \text{inv}\,\varphi}$ $V_j(\min)_p = 0$ when $s = s_o$ and $\beta_p = \beta_{pp}$	$d_p(\min, L) = 0$, when $m_g > m_g(\text{crit})$ note that: $0 < s < s_o$ and $0 < \beta_p \leq \beta_{pp}$ always

where

a = tooth addendum

$V_j(\text{Opt}, L)_p$ = Lowest jet velocity to obtain maximum impingement depth.

A minimum jet velocity condition exists for the pinion when $m_g > 1.0$ or $S \neq S_o$ and $\beta \neq \beta_{pp}$. This happens when V_j is less than required to place the jet head at position "A" in Fig. 2 as the leading edge of the top land of the pinion crosses the jet stream line. This position of the pinion can be calculated from:

$$\theta_{p3} = \cos^{-1}(r_s/r_o) - \text{inv}\,\varphi_{op} + \text{inv}\,\varphi \quad (11)$$

where

$$\text{inv}\,\varphi_{op} = \tan \varphi_{op} - \varphi_{op}$$

$$\varphi_{op} = \cos^{-1}(r_b/r_o) \text{ and}$$

$$r_s = r - S_p = r - [(r_o^2 + r^2 \cos^2 \beta_p)^{1/2} + r \sin \beta_p] \sin \beta_p \quad (12)$$

(See Figs. 1 and 2.)

Now the minumum jet velocity V_j that will wet the top land of the pinion (when $m_g > 1.0$) can be calculated from:

$$V_j(\min)_p = \frac{[(R_o^2 - R_s^2)^{1/2} - (r_o^2 - r_s^2)^{1/2}] \sec \beta_p\, \omega_p}{\varphi_{p1} - \varphi_{p3} + \text{inv}\,\varphi} \quad (13)$$

Note that when $m_g = 1$ or when $S = S_o$ or both, $V_j(\min)_p = 0$. The impingement depth at $V_j(\min)p$ is $d_p(\min, L) = 0$.

Equations 6 and 13 are shown in Table 1 with the other equations being developed herein and provide a form of graphical visibility based on the oil jet velocity scale (larger velocity at top of table).

Moving up the velocity scale to the next point of interest, there is a "constant impingement depth range" of oil jet velocity centered around $V_j = V_g = \omega_g R \sec \beta_p = \omega_p r \sec \beta_p$. The lower limit of this range of $V_j < \omega_p r \sec \beta_p$ can be calculated from:

$$V_j(\text{Opt, L}) = \frac{\omega_g (R_o^2 - R_s^2)^{1/2} \sec \beta_p}{\theta_{gl} + (\pi + 2B_g)/N_g} \tag{14}$$

This is the jet velocity that will barely get the stream head to a depth $d_p = a$. When $V_j = V_p = V_g = \omega_g r \sec \beta_p$ exactly, the pinion tooth is wetted on both the leading and trailing profiles down to the pitch line ($d_p = a$).

A selection or specification for V_j must be kept within the bounds of Equation 13 and $\omega_p r \sec \beta_p$ if impingement on the leading side of the tooth profile is required.

Development of Primary Formulae for the Generalized Gear Case ($0 \leqslant S \leqslant S_o$).

This sequence of events can be seen by looking at Figs. 2, 4 and 5 for the gear when $V_j < \omega_g R \sec \beta_p$. The jet stream is initially chopped by the pinion tooth (2) at "A" in Fig. 2, when the pinion is in the position θ_{p3}. At this time the gear tooth (3), where impingement will take place, is in position θ_{g3}, which can be calculated from Fig. 2:

$$\theta_{g3} = (\theta_{p3}/m_g) + \pi/N_g + 2\,B_g/N_g - \text{inv}\,\varphi \tag{15}$$

where:

N_g = Number of teeth in gear = $2\,P_d R$
B_g = Backlash for gear at $P_d = 1$ or $b_g\,P_d$
b_g = Backlash for gear (actual size), usually neglected.

As can be seen in Fig. 4, the pinion tooth (2) goes off and leaves the jet stream head and stream is subsequently chopped again at its tail end by the gear leading tooth profile (3) at the top land, as shown at "A" in Fig. 4. At this time the gear position can be calculated from:

$$\theta_{g4} = \cos^{-1}(R_s/R_o) - \text{inv}\,\varphi_{og} \tag{16}$$

The *intermediate* position of the jet *head* here is at

$$L_{ig} = (r_o^2 - R_s^2)^{1/2} \sec \beta_p = (\theta_{g3} - \theta_{g4})\,V_j/\omega_g \tag{17}$$

From here the jet head continues to fly toward the common line of centers at PP and the gear tooth (3) rotates until the leading profile intersects the head positions at "A" in Fig. 5 at impingement distance L_g. At this time the gear has rotated to the angular position calculated from:

$$\theta_{g5} = \tan^{-1}\left(\frac{L_g \cos \beta_p}{R + L_g \sin \beta_p}\right) - \text{inv}\,\varphi_{g5} \tag{18}$$

where:

$$\text{inv}\,\varphi_{g5} = \tan\varphi_{g5} - \varphi_{g5}$$

$$\varphi_{g5} = \cos^{-1} \frac{R_b}{[(R + L_g \sin \beta_p)^2 + (L_g \cos \beta_p)^2]^{1/2}} \tag{19}$$

The *analysis* solution for the gear is similar to, but somewhat more complicated than for the pinion alone. Using Equation 6 first solve explicitly for the pinion jet velocity V_{jp} as a function of the *selected* pinion impingement depth d_p. Then, because a given "gear mesh" must have a common jet velocity V_{jp}, the gear impingement depth d_g is solved for implicitly by first solving iteratively for the impingement distance L_g from Figs. 2, 4 and 5.

$$[(r_o^2 - r_s^2)^{1/2} \sec \beta_p - L_g]\omega_g = (\theta_{g3} - \theta_{g5})\,V_{jp} \quad \text{then} \tag{20}$$

$$d_g = R_o - [(R + L_g \sin \beta_p)^2 + (L_g \cos \beta_p)^2]^{1/2} \tag{21}$$

for $V_j(\min)_p < V_j < V_j(\text{Opt, L})_p$ and

$$d_g = a = \frac{1 \pm \Delta N/2}{P_d} \tag{22}$$

for $V_j(\text{Opt, L})_g \leqslant V_j$

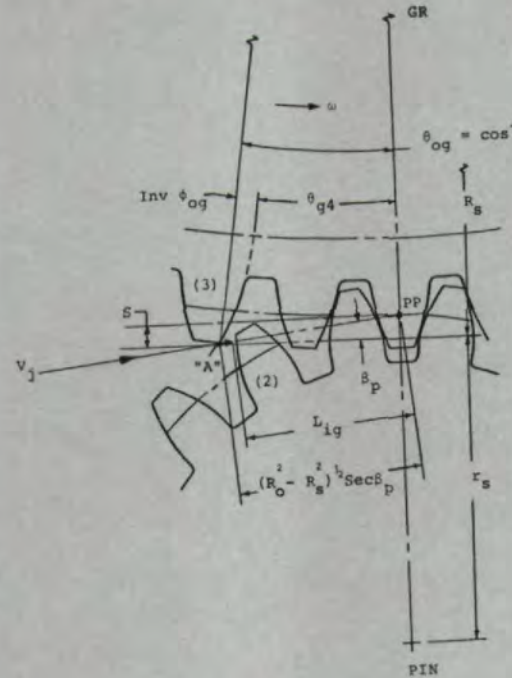

Fig. 4

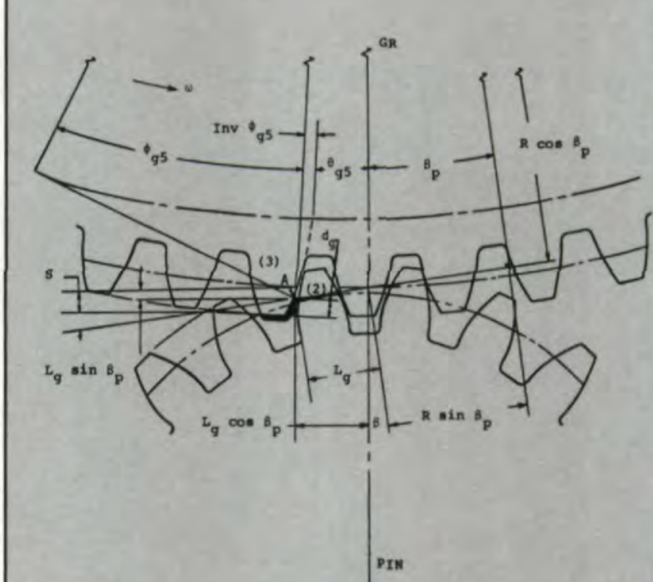

Fig. 5

where $V_j(\text{Opt}, L)_g$ is defined mathematically later.

The *design* solution for the gear is similar to the pinion, except more complex due to the boundary conditions imposed by the requirement to not allow jet velocities outside the range $V_j(\min)_g < V_j < V_j(\max)_g$ set by the pinion parameters. Noting again the equivalence of $t_f = t\omega$, the velocities inside this range can be calculated from:

$$V_j = \frac{\omega_g[(r_o^2 - r_s^2)^{1/2} \sec\beta_p - ((R_o - d_g)^2 - R^2 \cos^2\beta_p)^{1/2} + R \sin\beta_p]}{\theta_{g3} - \theta_{g5}} \quad (23)$$

with the additional restriction that

$$V_j(\min)_p = V_j(\min)_g < V_j < V_j(\text{Opt}, L)_g$$

to be explained later. Equation 23 is shown in Table 2 on a graphical velocity scale to give a perspective for this and the other velocity formulae relative to each other.

A minimum jet velocity condition also exists for the gear when $m_g > 1$, as shown above and explained in detail for the pinion using Fig. 2.

The initial position of the gear to establish this minimum velocity cycle, is at θ_{g1} in Fig. 1. The final or pinion chopping position at "A" in Fig. 2 for the gear may be calculated from:

$$\theta_{g2} = (\theta_{p3}/m_g) - (\pi/N_g) + 2\,B_g/N_g) \quad (24)$$

Therefore the minimum jet velocity V_j that can be allowed to avoid not wetting the pinion when $m_g > 1$, can be calculated using gear parameters from:

$$V_j(\min)_g = \frac{\omega_g[(R_o^2 - R_s^2)^{1/2} - (r_o^2 - r_s^2)^{1/2}] \sec\beta_p}{\theta_{g1} - \theta_{g2}} = 0 \quad (25)$$

when $S = S_o$, and the associated minimum impingement depth d_g is equal to zero (0).

Note that Equations 13 and 25 are equal:

$$V_j(\min)_p = V_j(\min)_g, \text{ and also}$$

$$\text{when } m_g = 1\ V_j(\min)_g = d_g(\min, L) = 0.$$

Moving up the velocity scale of Table 2 to the next point of interest, there is a constant impingement depth range of oil jet velocity for the gear also centered around $V_j = V_g = \omega_g R \sec \beta_p$. The lower limit of this range can be calculated from:

$$V_j(\text{Opt}, L)_g = \frac{\omega_g(r_o^2 - r_s^2)^{1/2} \sec\beta_p}{\theta_{p3}/m_g + (\pi/N_g + b_g/R)}$$

(continued on page 48)

Form Diameter of Gears

Harlan Van Gerpen
C. Kent Reece
Van Gerpen-Reece Engineering,
Cedar Falls, IA

One of the most frequently neglected areas of gear design is the determination of "form diameter". Form diameter is that diameter which specifies the transition point between the usable involute profile and the fillet of the tooth. Defining this point is important to prevent interference with the tip of the mating gear teeth and to enable proper preshave machining when the gear is to be finished with a shaving operation.

Gear designers that work only with standard or handbook gears have probably never been concerned with form diameter. The prescribed standard cutting tools have sufficient length to cut the fillet area so that generally no interference with the mating gear will occur, so long as finish hobbing or shaping is done. Many gear prints do not specifiy the form diameter for checking in the manufacturing process, apparently under the assumption that if a "standard" cutter is used, the form point will be acceptable. This is leaving too much to chance, particularly if the gear is undercut or if the gear is finished with a shaving or grinding operation.

For those gear designers that must focus on the strength of gear teeth or high contact ratio, and have abandoned standard gears to gain the advantage of custom designing, form diameter becomes extremely important. Designers of custom gears no longer have the comfort of having adequate clearance being provided as found in the handbook tables and soon realize that every possible avenue of interference must be investigated. However, these extensive mathematical calculations are no longer a hindrance because of the availability of inexpensive computers and gear design software.

Gaining the optimum gear tooth strength requires the fillet to blend as closely as possible to the active root end of the involute profile. Not only does this enhance the beam strength of the tooth, but also helps to provide material in the root area for some special applications, such as planet pinions, where the required bore diameter may threaten the strength of the root section.

If a gear is to be cut with a finishing hob (a hob without a protuberance), the equations given below are sufficient for gears that have no natural undercut.

$$\text{Form Radius} = \sqrt{\left(\frac{R - RR - C1}{\tan\phi}\right)^2 + (RR + C1)^2}$$

R = Generating pitch radius
RR = Root radius
C1 = Hob tip clearance
ϕ = Pressure angle (transverse)

(1)

For shaper-cut gears:

$$\text{Form Radius} = \sqrt{\left[\sqrt{CD^2 - BRT^2} - \sqrt{ORc^2 - BRc^2}\right]^2 + BRg^2}$$

$$BRT = BRc + BRg$$

CD = Center distance
BRc = Cutter base radius
BRg = Gear base radius
ORc = Cutter outside radius (minus tip clearance)

(2)

However, if the gear is to be shaved (or ground), then the fillet area becomes much less defined. Then it is necessary to use an exact definition of the preshave cutter and to explore the path of the tip of the cutter and how this path relates to the final "shaved" profile.

A gear is shaved by placing it in tight mesh with and at a small crossed axis angle to a shaving cutter, which resembles the gear, except that its teeth faces are serrated. As the two are rotated together, the serrations on the shaving cutter teeth remove a small amount of material from the involute profile of the gear. It is common practice to provide a "protuberance" on the tip of the preshave cutter to provide adequate relief to allow clearance in the gear root area for the tip of the shaving cutter tooth. If this is not provided, the

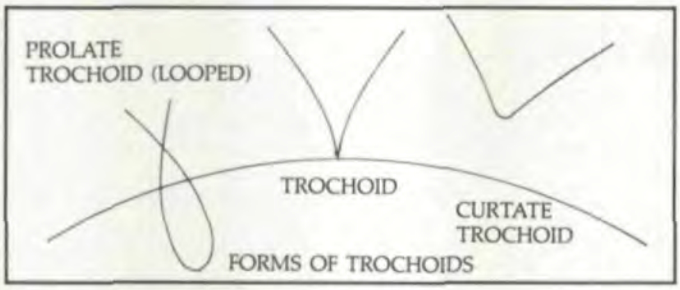

Fig. 1

shaving cutter may leave a "step" on the gear tooth profile near the root end of the involute profile where the tip of the mating gear will make contact. This may result in noise, wear and vibration.

Assuming the preshave cutter is a hob or basic rack shaped cutter, let us review the possible generating paths for different points on the cutter. We must consider the different possible trochoidal paths that the specific points on the preshave cutter will follow. If the gear is expected to operate at a pressure angle with another gear at about the same pressure angle as the cutter, then we can expect the tip of the cutter to extend below the pitch radius of the gear and execute a prolate or "looped" trochoid. Points further away from the cutter tip will have lesser "loops", and still further, the points that stay outside the pitch radius will execute a curtate trochoid. Equations which follow these trochoid curves provide the information for determining the form diameter. Examples of these trochoidal forms are given in Fig. 1.

The problem of form diameter with custom gears is that for increased strength it is common practice to operate with a mating gear at a much higher pressure angle than used with the cutter to generate the tooth. In other words, the operating pitch diameter is much larger than the generating pitch diameter. It is entirely possible that during the generation of the tooth, the tip of the cutter will not cross the generating pitch circle. This results in the tip components following curtate trochoid paths.

As the preshaved cutter is used to generate gears to operate at high pressure angles, the path of the protuberance more closely parallels the involute of the finished gear. This leads to the removal of part of the shaving stock that is expected to be present during the shaving operation. With no stock to remove, the surface is not cleaned up and will present a rough surface to the mating gear tooth tip. Therefore, the process of selecting an acceptable form diameter depends upon how much stock must be present for shaving. In some cases of excessive stock removal, the shaving cutter will act erratically. If the contact ratio with the gear is low, part of the time the shaver will ride on the thinner stock section, introducing a second involute profile with a larger base radius.

It is our practice to specify the minimum amount of shaving stock to be provided in the fillet as gear design input. The computation then provides two diameters – the point of maximum relief and the diameter where adequate shaving stock will exist. The outside diameter of the shaving cutter must blend between these two diameters; the closer to the maximum relief, the better.

Another area of exploration relates to the shape of the tip of the cutter. The question is what is the shape of the transition zone on the tip of the hob between the tip radius and the involute producing section of the cutter? With a "looped" trochoid condition we can rely on the clearance point on the hob as the critical point in computing the form diameter. However, when the tip executes a curtate trochoid, the hob transition zone may affect the fillet generation. Many cutters use a secondary involute, perhaps 10° different than the primate involute, as a blend with the tip radius. During the tooth generation process this may actually be forming the final shape of the preshaved profile. The design computation must compute this condition if the form diameter is allowing for shaving stock.

If the tooth is being generated with a shaper cutter, our options are rather limited. The same general procedure is used to determine the existence of the form diameter. However, the transition zone on the shaper between the tip clearance point and the involute profile is rarely defined by the cutter suppliers, so we are limited to only exploring the path of the clearance point in determining the existence of shaving stock and establishing the form diameter.

The method of computation is an iterative procedure following the path of the clearance point on the cutter and comparing its distance from the center of a gear tooth with the distance of a finished involute. When these distances are the same or different by the predetermined small amount, that diameter is the form diameter, and one is now assured that the shaving cutter will have stock to remove and provide a smooth surface. The designer must have an understanding with the manufacturer concerning the minimum stock required.

Figs. 2 and 3 and associated equations are included to provide more detail of a procedure used to define the form diameter for shaved gears using protuberance cutters. In Fig. 2 one can calculate from the tight meshed condition the tooth space on the gear, and then establish the hob tooth thickness at the generating pitch line.

Since the clearance point of the hob will be doing the critical cutting in the area where the fillet joins the involute, it is the trochoid of this point that must be followed. To do this, the engineer needs to know the dimension "B", the distance from the generating pitch line to the clearance point.

Some hob suppliers do not use a secondary involute, but provide a clearance dimension on the hob print. "B" then is the distance to this given clearance point from the generating pitch line.

Many hob suppliers provide a protuberance height (PH, Fig. 2) that is slightly greater than the amount "thin" of the cutter tooth. This must be compensated for because it provides additional undercut from the area of the involute/fillet blend.

This discussion is limited to the study of gears with low operating pressure angles or gears where the clearance point executes a "looped" trochoid. With higher operating pressure angles, the trochoid may be curtate. Under these conditions, the fillet is generated as the cutter "rolls into" the root rather than as it "rolls out" of the root.

As previously mentioned, the secondary involute may remove the "stock" in the blend area. This involute, being at a different pressure angle, operates from a different base circle. It is necessary to calculate the tooth thickness being cut by this part of the cutter, compare with the other computed form diameters and select the larger number for the form diameter.

Fig. 3 and associated equations illustrate the mathematical

Fig. 2

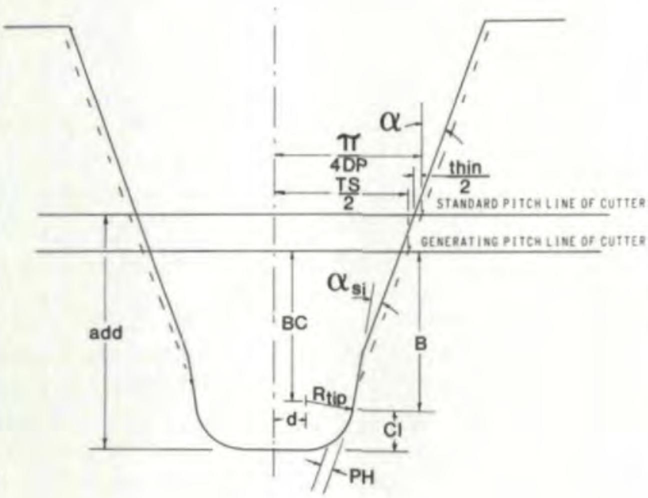

$$\frac{TS}{2} = \frac{\pi}{2\,DP} - \frac{TTg}{2}$$

$$d = \frac{\pi}{4\,DP} - (add - R_{tip}) \times TAN\,\alpha$$

$$-\frac{R_{tip} - \left(PH - \frac{thin}{2} \times COS\,\alpha\right)}{COS\,\alpha}$$

$$BC = add - R_{tip} - \frac{\left(\frac{\pi}{4\,DP} - \frac{TS}{2}\right)}{TAN\,\alpha}$$

$$B = BC + R_{tip} \times SIN\,(\alpha - \alpha_{si})$$

$$B = add - C1 - \frac{\frac{\pi}{4DP} - \frac{TS}{2}}{TAN\,\alpha}$$

DP = Diametral Pitch
TTg = Gear Tooth Thickness at Pitch Radius

Fig. 3

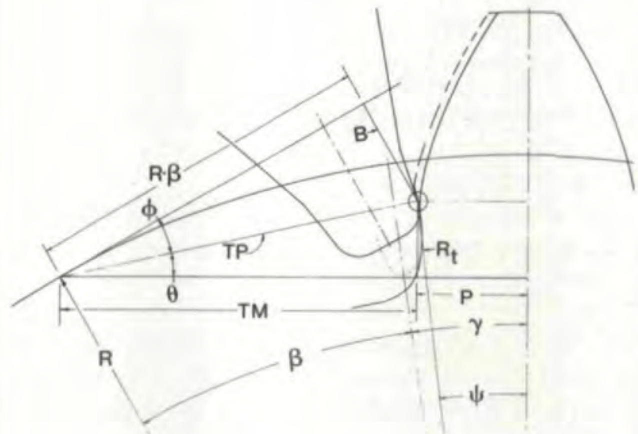

$$\gamma = \frac{\frac{CP}{2} - d - R_{tip} \times COS\,(\alpha - \alpha_{si})}{R}$$

$$\phi = ATAN\left(\frac{B}{R \times \beta}\right)$$

$$\theta = \beta + \gamma - \phi$$

$$TP = \sqrt{B^2 + (R \times \beta)^2}$$

$$TM = TP \times COS\,\theta$$

$$P = R \times SIN\,(\gamma + \beta) - TM$$

$$R_t = \sqrt{(R - B)^2 + (R \times \beta)^2}$$

$$\psi = ASIN\left(\frac{P}{R_t}\right)$$

$$TTC = R_t \times \psi$$

CP = Circular Pitch
TTC = Circular Distance of Cutter Path from Tooth Centerline

process to be used in following the path of the clearance point trochoid. The angle β is adjusted until the desired configuration is achieved. The form diameter of a non-shaved gear is the diameter where the involute begins. The form diameter of a shaved (or ground) gear is the diameter of the point on the tooth where adequate shaving stock is available.

This procedure is also applicable to helical gears if done in the normal plane with a derived "virtual" gear.

The above procedure is also useful in determining whether a shaving cutter already on the shelf can be used to shave a new gear. The computations can also include the modifications that can be made to an existing shaving cutter so that obsolete cutters can be made usable again.

Appendix — Sample Calculations For Finding Form Diameter of Gears

Given: Diametral Pitch	(DP)	=	5.0
Hob Pressure Angle	(α)	=	20°
Hob Addendum	(add)	=	.27
Hob Tip Radius	(R_{tip})	=	.05
Amount Thin	(thin)	=	.005
Protuberance Height	(PH)	=	.003
Secondary Involute	(αsi)	=	10°
Teeth in Gear		=	16
Pitch Radius	(R)	=	1.600
Gear Tooth Thickness at R	(TTg)	=	.3400

From Fig. 2:

$$\frac{TS}{2} = \frac{\pi}{2\ DP} - \frac{TTg}{2} = \frac{\pi}{10} - \frac{.34}{2} = .14416 \qquad (1)$$

$$d = \frac{\pi}{4\ DP} = (add - R_{tip})\ TAN\ \alpha$$

$$- \frac{R_{tip} - \left(PH - \frac{thin}{2} \times COS\ \alpha\right)}{COS\ \alpha}$$

$$= .15708 - .08007 - .05252 = .02449 \qquad (2)$$

$$BC = add - R_{tip} - \frac{\left(\frac{\pi}{4\ DP} - \frac{TS}{2}\right)}{TAN\ \alpha}$$

$$= .27 - .05 - .0355 = .18450 \qquad (3)$$

$$B = BC + R_{tip} \times SIN\ (\alpha - \alpha_{si})$$

$$= .18450 + .05\ SIN\ (20° - 10°) = .19318 \qquad (4)$$

From Fig. 3:

$$\gamma = \frac{\frac{CP}{2} - d - R_{tip} \times COS\ (\alpha - \alpha_{si})}{R}$$

$$= \frac{.31416 - .02449 - .050\ (COS\ 10°) = .15027}{1.6} \qquad (1)$$

Assume $\beta = .34$ radians

$$\phi = ATAN \left(\frac{B}{R \times \beta}\right)$$

$$= ATAN \left(\frac{.19318}{1.6 \times .34}\right) = .34122 \qquad (2)$$

$$\theta = \beta + \gamma - \phi = .34 + .15027 - .34122$$

$$= .14905 \qquad (3)$$

$$TP = \sqrt{B^2 + (R \times \beta)^2} = \sqrt{.19318^2 + (1.6 \times .34)^2}$$

$$= .57728 \qquad (4)$$

$$TM = TP \times COS\ \theta = .57728\ COS\ (.14905)$$

$$= .57088 \qquad (5)$$

$$P = R \times SIN\ (\gamma + \beta) - TM$$

$$= 1.6\ SIN\ (.49027) - .57088 = .18250 \qquad (6)$$

$$R_t = \sqrt{(R - B)^2 + (R \times \beta)^2}$$

$$= \sqrt{(1.40682\ )^2 + (1.6 \times .34)^2} = 1.5083 \qquad (7)$$

$$\psi = ASIN \left(\frac{P}{R_t}\right) = ASIN \left(\frac{.18250}{1.5083}\right) = .12129 \qquad (8)$$

(continued on page 44)

CLASSIFIED

Rates: Classified Display—per inch (minimum 3) **1X**-$130, **3X**-$120, **6X**-$110. Type will be set to advertiser's layout or *Gear Technology* will set type at no extra charge. **Word Count:** 35 characters per line, 7 lines per inch.

Payment: Full payment must accompany classified ads. Mail copy to *Gear Technology*, P.O. Box 1426, Elk Grove Village, IL 60009. **Agency Commission:** No agency commission on classifieds.

Material Deadline: Ads must be received by the 25th of the month, two months prior to publication. **Acceptance:** Publisher reserves the right to accept or reject classified advertisements at his discretion.

FORM DIAMETER . . .
(continued from page 41)

$$TT_{circ} = R_t \times \psi = 1.5083 \times .12129 = .18295 \qquad (9)$$

½ tooth thickness of finished tooth at R_t is:

$$TT = R_t \left(\frac{TTg}{2\ R} + \text{INV}\ \phi_1 - \text{INV}\ \phi_2 \right)$$

$$= 1.5083 \left(\frac{.34}{3.2} + .0149044 - .00017 \right) = .18248 \qquad (10)$$

At this condition the hob clearance point is leaving about .0005" of finishing stock for shaving. More shaving stock will be available if β is increased, with a slight increase in R_t, the maximum form diameter.

AUTHORS:

HARLAN VAN GERPEN *has 28 years of experience at the John Deere Product Engineering Center in Waterloo, Iowa, where he served as manager of technical services and a principal engineering specialist. He is a licensed professional engineer in the State of Iowa and a member of the ASAE, where he is a member of the Research Committee and the Instrumentation and Controls Committee. He is also a member of the SAE Education and Human Factors Committees. Mr. Van Gerpen holds a master's degree in electrical engineering from the University of Illinois.*

CARROLL K. REECE *worked for the John Deere Product Engineering Center, Waterloo, Iowa, as an engineering design analyst and supervisor in the mechanical elements department. He has served for 25 years on the ANSI-B92 National Spline Standards Committee and for 18 years on both the ISO TC 32 International Spline Standards Committee and the ANSI-B6 National Gear Standards Committee. He holds a master's degree in agricultural engineering from Kansas State University and is a licensed professional engineer in the State of Iowa.*

VIEWPOINT

20° FULL DEPTH INVOLUTE SYSTEM (ASA-B 6b-1933)

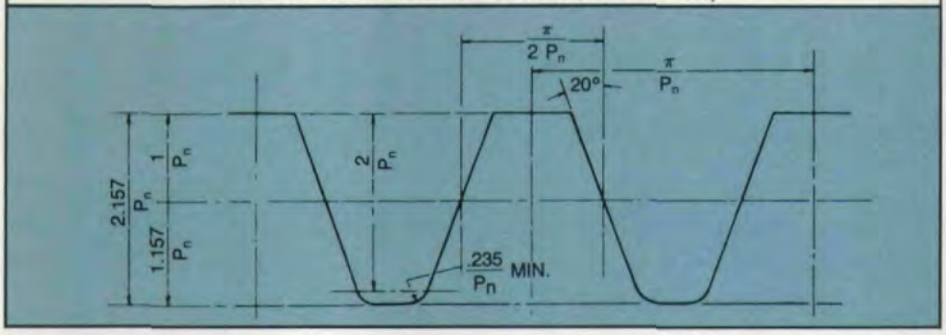

Dear Editors:

Regarding the tables for small pinions and internal gears for internal gear drives, published in the Mar-Apr issue on pp. 38-48, the values given are for the plane of rotation or transverse plane. They apply to all helix angles. As these values are for 1 diametral pitch, it is necessary to divide the values by the diametral pitch to obtain the numerical value. It is also necessary to divide values by the cosine of the helix angle.

Another way of expressing it would be to say that for helical gears, when the NORMAL 1 DP rack is specified, the 1 DP values are divided by the normal diametral pitch, Pn. When the axial or transverse rack is specified, then the values are divided by the transverse diametral pitch, P1, which is equal to the normal diametral pitch times the cosine of the helix angle, ψ, or $P1 = Pn^*\cos(\psi)$. Thus, where the pitch radius is given for a 5 tooth pinion in the table as 2.5 inches, for a 15° helix angle, the value would be 2.588.

It might have helped to clarify this if the basic rack form, enclosed, had been included.

Eliot K. Buckingham
President
Buckingham Associates, Inc.

Dear Editors:

The article by Lewicki (Vol. 6, No. 2, p. 6) looks very good. Your magazine gets wide circulation, and it is very attractive. We hear directly from readers who see our articles there. I appreciate the opportunity for our work to be presented in your magazine.

Dr. John J. Coy
Mechanical Systems Technology Branch
NASA Lewis Research Center
Cleveland, OH

INTO-MESH LUBRICATION . . .

(continued from page 36)

TABLE 2. - EQUATIONS FOR OIL JET VELOCITY AND GEAR IMPINGEMENT DEPTH FOR PITCH LINE AND LOWER OIL JET VELOCITIES

Relative velocity scale	Oil jet velocity	Pinion impingement depth
Pitch line and slightly lower	$V_j = \omega_g R \sec \beta$ (at pitch point) $V_j(\text{opt}, L) = \dfrac{\omega_p (r_o^2 - r_s^2)^{1/2} \sec \beta_p}{r_{p3} + (\pi + 2\,B_p)/N_p}$	$d_g = a = \dfrac{1}{P_d} + \dfrac{\Delta N}{2P_d}$
Less than pitch line velocity down to where oil jet starts to miss the gear	$V_j = \dfrac{\omega_g \{(r_o^2 - r_s^2)^{1/2} \sec \beta_p - [(R_o - d_g)^2 - (R \cos \beta_p)^2]^{1/2} - R \sin \beta_p\}}{\theta_{g3} - \theta_{g5}}$ V_j given	d_g given $L_g = [(R_o - d_g)^2 - R^2 \cos^2 \beta_p]^{1/2} - R \sin \beta_p$ Iterate L_g from: $[(r_o^2 - r_s^2)^{1/2} \sec \beta_p - L_g]\omega_g = (r_{g3} - r_{g5})V_j$ then $d_g = R_o - [(R + L_g \sin \beta_p)^2 + (L_g \cos \beta_p)^2]^{1/2}$
Critical low velocity to miss the gear	$V_j(\min)_g = \dfrac{\omega_g[(R_o^2 - R_s^2)^{1/2} - (r_o^2 - r_s^2)^{1/2}]\sec \beta_p}{r_{g1} - r_{g2}}$ $V_j(\min)_g = 0$ when $S = S_o$ and $\beta_p = \beta_{pp}$ or when $m_g = 1$	$d_g(\min, L) = R_o - \{[R + L_g(\min)\sin \beta_p]^2 + [L_g(\min)\cos \beta_p]^2\}^{1/2}$ $d_g(\min, L) = 0$ when $S = S_o$ and $\beta_p = \beta_{pp}$ or when $m_g = 1$

$$= \frac{\omega_p (r_o^2 - r_s^2)^{1/2} \sec \beta_p}{\theta_{p3} + (\pi + 2\,B_p)/N_p} \tag{26}$$

(See Fig. 2.)

Notice that this jet velocity will barely get the jet stream head initiated at "A" on tooth (2) to a depth $d_g = a$ or the gear tooth (3) at PP. Also when $V_j = V_g = \omega_j R \sec \beta_p$ exactly, the gear tooth is wetted on both sides of the tooth profiles down to the pitch line ($d_g = a$).

Summary

An analysis was conducted for into-mesh oil jet lubrication with an arbitrary offset and inclination angle from the pitch point for the case where the oil jet velocity is equal to or less than the pitch line velocity. The analysis includes the case for the oil jet nozzle offset from the pitch point in the direction of the pinion and where the oil jet is inclined to intersect the common pitch point. Equations were developed for the minimum oil jet velocity required to impinge on the pinion or gear and the optimum oil jet velocity required to obtain the best lubrication condition of maximum impingement depth and gear tooth cooling. The following results were obtained.

1. The optimum operating condition for best lubrication and cooling is provided exactly when $V_j = V_g = \omega_p r \sec \beta_p = \omega_g R \sec \beta_p$, so that both sides of the pinion and gear will be wetted and, therefore, cooled.

2. When the jet velocity is slightly less than the gear velocity (V_j Opt L) $\leqslant V_j < V_g$) the loaded side of the driver is forward and receives the best cooling.

3. As the jet velocity is much less than the gear pitch line velocity, $V_j << [V_j(\text{Opt}, L)] < V_g$, the impingment depth is considerably reduced. This may result in the pinion being completely missed with no primary pinion cooling provided.

References

1. AKIN, L., MROSS, J. and TOWNSEND, D. "Theory for the Effect of Windage on the Lubricant Flow in the Tooth Spaces of Spur Gears," *Trans. ASME, J. Engr. for Industry*, Vol. 79, Ser. B, No. 4, 1975, pp. 1266-1283.
2. AKIN, L. and TOWNSEND, D. "Study of Lubricant Jet Flow Phenomena in Spur Gears," *Trans. ASME, J. Lubrication Tech.*, Vol. 97, Ser. F, No. 2, 1975, pp. 283-288.
3. TOWNSEND, D. and AKIN, L. "Study of Lubricant Jet Flow Phenomena in Spur Gears — Out-of-Mesh Condition," *Trans. ASME, J. Mech. Design*, Vol. 100, No. 1, Jan. 1978, pp. 61-68.
4. TOWNSEND, D. and AKIN, L. "Analytical and Experimental Spur Gear Tooth Temperature as Affected by Operating Variables," *Trans. ASME, J. Mech. Design*, Vol. 103, No. 4, Jan. 1981, pp. 219-226.
5. WINTER, AREND de, and BLOK, H. "Fling-Off Cooling of Gear Teeth," *Trans. ASME, Engr. for Industry*, Vol. 96, Ser. B, No. 1, 1974, pp. 60-70.
6. AKIN, L, and TOWNSEND, D. "Cooling of Spur Gears with Oil Jet Directed into the Engaging Side of Mesh at Pitch Point," *JSME — Proc. of Inter. Symposium on Gearing and Power Transmissions*, 1981, Vol. 1, b-4, pp 261-274.
7. FUJITA, K., OBATA,, F. and MATSUO, K. "Behavior of Lubricating Oil Into the Meshing Parts of Spur Gears — The Case of Jet Lubrication onto the Engaging Side," *J. of Japan Society of Lubrication Engineers*, Vol. 19, No. 6, 1974, pp. 437-447.
8. FUJITA, K. and OBATA, F. "The Influence of Lubricating Oil on the Scoring Resistance of Spur Gears," *J. of Japan Society of Lubrication Engineers*, Vol. 18, No. 5, 1973, pp. 383-393.

Acknowledgement: *Reprinted courtesy of American Society of Mechanical Engineers, from their Winter Annual Meeting, Phoenix, AZ, November 15-19, 1982 and* ASME Journal of Mechanisms, Transmissions, and Automation in Design, *Vol. 105, Dec., 1983, pp. 713-724. Also published as NASA Technical Memorandum, 83040.*

SHAVE OFF THAT EXPENSE FROM YOUR PRODUCTION COST WITH A MITSUBISHI.

Mitsubishi's CNC gear shaving machine assures you high productivity with setup time reduced to 1/8 of the conventional type shavers. Positioning of work-piece and cutter, diagonal angle setting are all controlled automatically from the CNC.

Cutting conditions are stored in memory for ease of operation. Sturdy construction and thermally balanced structure maintains high accuracy.

For more details please contact our sales engineer at our Bensenville office.

DIASHAVE
FA30CNC

MITSUBISHI
HEAVY INDUSTRIES, LTD.
5-1, Marunouchi 2-chome, Chiyoda-ku, Tokyo, Japan
Cable Address: HISHIJU TOKYO

Mitsubishi Heavy Industries America, Inc.
873 Supreme Drive, Bensenville, IL 60160 Phone: (312) 860-4220

Mitsubishi International Corporation
873 Supreme Drive, Bensenville, IL 60160 Phone: (312) 860-4222

CIRCLE A-32 ON READER REPLY CARD